ARH directs megalin to the endocytic recycling compartment to regulate its proteolysis and gene expression

Mehul Shah, Oscar Y. Baterina Jr., Vanessa Taupin, and Marilyn G. Farquhar

Department of Cellular and Molecular Medicine, University of California, San Diego, La Jolla, CA 92093

Receptors internalized by endocytosis can return to the plasma membrane (PM) directly from early endosomes (EE; fast recycling) or they can traffic from EE to the endocytic recycling compartment (ERC) and recycle from there (slow recycling). How receptors are sorted for trafficking along these two pathways remains unclear. Here we show that autosomal recessive hypercholesterolemia (ARH) is required for trafficking of megalin, a member of the LDL receptor family, from EE to the ERC by coupling it to dynein; in the absence of ARH, megalin returns directly to the PM from EE via the connecdenn2/Rab35 fast recycling pathway. Binding of ARH to the endocytic adaptor AP-2 prevents fast recycling of megalin. ARH-mediated trafficking of megalin to the ERC is necessary for γ-secretase mediated cleavage of megalin and release of a tail fragment that mediates transcriptional repression. These results identify a novel mechanism for sorting receptors for trafficking to the ERC and link ERC trafficking to regulated intramembrane proteolysis (RIP) and expression of megalin.

Introduction

Clathrin-mediated endocytosis is initiated when a ligand binds to its receptor at the plasma membrane (PM), and the bound receptor is sorted into clathrin-coated vesicles by endocytic adaptor proteins (Traub, 2009; Kelly and Owen, 2011; McMahon and Boucrot, 2011). The internalized receptor is delivered to early sorting endosomes (EE) that sort cargo for targeting to different destinations (Platta and Stenmark, 2011). For example, the EGF receptor is mainly sorted for lysosomal degradation (Scita and Di Fiore, 2010), whereas the LDL receptor (LDLR), transferrin receptor (TfR), and the major histocompatibility complex II (MHC II) are recycled back to the PM (Daro et al., 1996; Walseng et al., 2008). MHC II and a pool of TfR recycle directly from the EE via the fast recycling pathway (Daro et al., 1996; Walseng et al., 2008), whereas some receptors such as megalin (Nagai et al., 2003) and TfR (Ullrich et al., 1996; Ren et al., 1998) take the slow recycling pathway in which they are sorted in EE and targeted to the endocytic recycling compartment (ERC) before returning to the PM (Grant and Donaldson, 2009). A number of proteins (e.g., Rab GTPases, sorting nexins) are known to facilitate trafficking of receptors between EE, the ERC, and the PM (Grant and Donaldson, 2009; Hsu and Prekeris, 2010). Similarly, a number of motifs, notably PDZ-binding motifs that mediate recycling of receptors, have been identified (Hanyaloglu and von Zastrow, 2008; Hsu et al., 2012). However, no sorting mechanisms or motifs involved in directing receptors from EE to the ERC have been reported, and the physiological significance of delivery of some receptors to the ERC before being recycled to the PM remains unknown.

We previously discovered that megalin (gp330, LRP2), a member of the LDLR family, follows the slow recycling pathway through the ERC (Saito et al., 1994; Nagai et al., 2003). Megalin is expressed in many epithelial cells (renal proximal tubule, thyroid, parathyroid) and binds a number of ligands (Christensen and Verroust, 2002; Birn and Christensen, 2006)

Correspondence to Marilyn G. Farquhar: mfarquhar@ucsd.edu

Abbreviations used in this paper: ARH, autosomal recessive hypercholesterolemia; CLASP, clathrin-associated sorting protein; DHC, dynein heavy chain; DIC, dynein intermediate chain; EE, early endosomes; ERC, pericentriolar recycling compartment; IF, immunofluorescence; IP, immunoprecipitation; LDLR, low-density lipoprotein receptor; M4, mini-megalin receptor; MCTF, megalin cytoplasmic tail fragment; MEF, mouse embryonic fibroblast; MESNA, 2-mercaptoethanesulfonic acid; MHC II, major histocompatibility complex II; MICD, megalin intracellular domain; MT, megalin tail; NHE3, sodium hydrogen exchanger 3; NTA, nitrilotriacetic acid; PM, plasma membrane; PTB, phosphotyrosine binding; PTD, peptide transduction domain; RIP, regulated intramembrane proteolysis; shRNA, short hairpin RNA; TfR, transferrin receptor; TR-Tf, Texas red–transferrin; wt, wild type.

The Rockefeller University Press $30.00
J. Cell Biol. Vol. 202 No. 1 113–127
www.jcb.org/cgi/doi/10.1083/jcb.201211110

and has important physiological roles in development and in kidney physiology and pathology. Developmental anomalies occur in patients with megalin mutations and in *megalin*$^{-/-}$ mice (Willnow et al., 1996; Kantarci et al., 2007); the latter also experience loss of low molecular weight proteins and other metabolites in the urine (Cui et al., 1996; Leheste et al., 1999). Despite the many important roles of megalin, the mechanisms that regulate its endocytic trafficking are not fully understood.

Megalin interacts with a number of proteins via conserved motifs in its cytoplasmic tail, which includes two FXNPXY motifs (Saito et al., 1994). We previously reported that the first FXNPXY motif of megalin binds to the phosphotyrosine-binding (PTB) domain of the autosomal recessive hypercholesterolemia (ARH) protein (Nagai et al., 2003), and the second FXNPXY motif was shown to interact with the PTB domain of Dab-2 (Oleinikov et al., 2000). ARH and Dab-2 are considered to be clathrin-associated sorting proteins (CLASPs; Traub, 2009), as they couple receptors to the clathrin machinery. ARH accomplishes this by simultaneously engaging FXNPXY motifs within cytoplasmic tails of receptors via its N-terminal PTB domain and clathrin and AP-2 via motifs within its C terminus (Garcia et al., 2001; He et al., 2002; Mishra et al., 2002, 2005). Consistent with ARH's role as a CLASP, ARH$^{-/-}$ mice as well as patients with autosomal recessive hypercholesterolemia, a genetic disorder in which ARH is mutated, show reduced internalization of the LDL–LDLR complex (Garcia et al., 2001; Jones et al., 2003). ARH is indispensable for LDL uptake at the systemic level, but in certain cell types (e.g., fibroblasts) Dab-2 has been shown to compensate for the absence of ARH (Keyel et al., 2006; Maurer and Cooper, 2006).

We previously found that ARH accompanies megalin throughout its entire endocytic recycling itinerary from the PM to EE to the ERC and back to the PM (Nagai et al., 2003), suggesting that ARH may have additional roles in megalin trafficking. We found later that ARH also interacts with subunits of the dynein motor (Lehtonen et al., 2008). Because dynein mediates transport of cargo along microtubules toward the cell center, this suggested that ARH might facilitate trafficking of megalin along microtubules. Here we report that ARH is required for trafficking of megalin from EE to the ERC, and we have defined the mechanisms by which it mediates this function. We further demonstrate that ARH-mediated trafficking of megalin to the ERC is necessary for the regulated intramembrane proteolysis (RIP) of megalin's cytoplasmic tail and regulation of megalin gene expression.

Results

ARH knockdown inhibits trafficking of megalin to the ERC

To study the role of ARH in megalin trafficking, we made two Cre-inducible, ARH knockdown L2 cell lines (L2-sh3 and L2-sh4). We used L2 rat yolk sac cells because they express high levels of endogenous megalin. Both cell lines showed >80% knockdown of ARH compared with a control cell line (L2-Luc) after Cre-mediated recombination (Fig. 1 A). We tested the effect of ARH knockdown on megalin trafficking in these cells using an assay developed previously (Nagai et al., 2003). Cells were placed on ice to stop endocytosis and incubated with megalin 20B mAb, a nonperturbing antibody that binds to the ectodomain of megalin; after warming, the antibody-bound megalin follows the natural endocytic recycling pathway of megalin. As shown previously for wild-type (wt) L2 cells, in L2-Luc controls 20B labeled the surface pool of megalin before warming (Fig. 1 B; 0 min), and when the cells were switched to 37°C and resumed endocytosis, megalin trafficked from the PM to EEA1-positive EE within 2 min (Fig. 1, B and C). By 15 min virtually all of the internalized megalin was at the ERC as determined by colocalization with Rab11 (Fig. 1, B and D), an ERC marker (Ullrich et al., 1996). In L2-sh3 and L2-sh4 cells megalin arrived at EE within 2 min (Fig. 1, B and C) as in controls; however, it did not reach the ERC at 15 min and remained in scattered peripheral vesicles where it partially colocalized with EEA1 but not Rab11 (Fig. 1, B and D). These findings suggest that ARH is not required for internalization of megalin from the PM, but it is required for megalin trafficking from EE to the ERC. Similar results were obtained when cells were incubated with 20B mAb for 2 min at 37°C instead of on ice (not depicted). The defect in the arrival of megalin at the ERC was not due to reduced levels of megalin at the PM, as both ARH-depleted cells and controls showed comparable levels of 20B bound to the cell surface (Fig. 1 B). Flow cytometry confirmed equal 20B mAb cell surface labeling in all three cell lines (not depicted). Moreover, biotinylation assays showed no significant difference in internalization of M4-GFP, a GFP-tagged megalin minireceptor (M4) (Fig. S1). By immunoelectron microscopy there was no notable morphological difference in the tubular organization of the ERC in L2-sh3 cells compared with controls, but there was reduced labeling of megalin at the ERC (Fig. S2).

To determine whether the effect of ARH knockdown on trafficking from EE to the ERC is specific for megalin, we performed simultaneous uptake of megalin and Texas red–transferrin (TR-Tf). Transferrin-bound TfR also traffics to the ERC after internalization; however, unlike megalin, TfR does not possess an FXNPXY motif and does not bind ARH, and hence ARH depletion would not be expected to affect TfR trafficking to the ERC. We found that in L2-Luc controls, both megalin and transferrin colocalized in the ERC at 15 min; by contrast, in L2-sh3 ARH knockdown cells TR-Tf arrived at the ERC whereas megalin remained scattered in peripheral vesicles (Fig. 1 E). 15.9 ± 8.7% of the L2-sh3 cells showed colocalization of megalin with TR-Tf compared with 97.4 ± 0.8% (mean ± SEM, $n = 3$) in L2-Luc controls. These results indicate that ARH knockdown is specific for megalin and does not lead to a general defect in trafficking to the ERC.

To rule out that the defect in trafficking in ARH knockdown cells was due to off-target effects of RNAi silencing, we performed rescue assays by delivering 6xHis-tagged ARH (wtARH-His) into L2-sh3 cells. wtARH-His was complexed with PTD-NTA, a conjugate of the peptide transduction domain (PTD) from HIV Tat protein that can transduce cells (June et al., 2010). wtARH-His (1 µM) complexed with PTD-NTA restored cellular levels of ARH to near-endogenous levels in L2-sh3 cells (Fig. 2 A, lanes 9 and 10) and also successfully restored

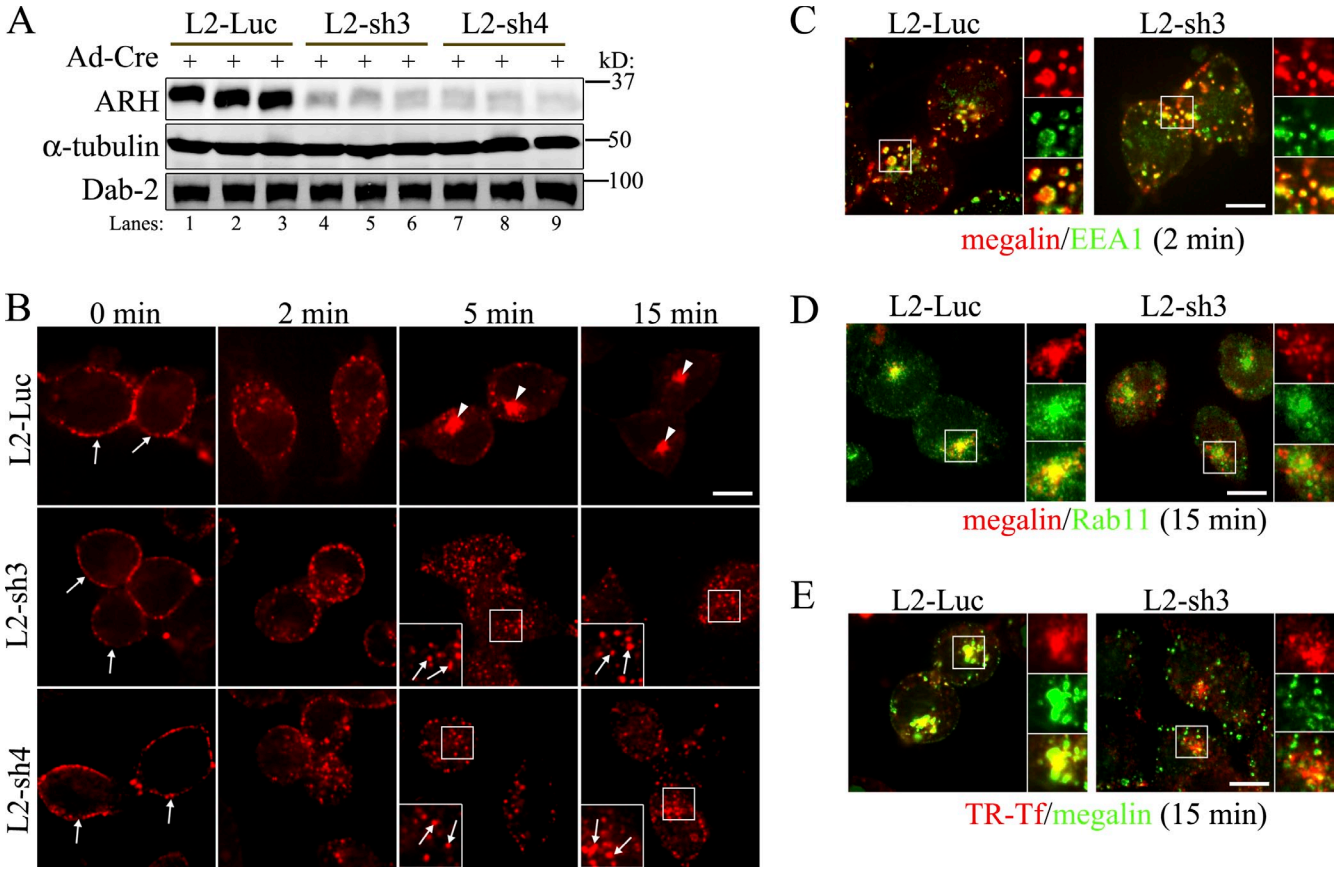

Figure 1. **ARH knockdown inhibits megalin trafficking from EE to the ERC.** (A) Immunoblotting showing ARH levels are decreased (83%) in cells expressing ARH shRNAs (lanes 4–9) compared with L2-Luc cells (lanes 1–3) expressing control shRNA. shRNA expression was induced in L2-Luc, L2-sh3, and L2-sh4 cells by Ad-Cre, and 60 h later cells were lysed and analyzed by immunoblotting for the indicated proteins. (B) IF of megalin trafficking after ARH knockdown. Megalin (red) localizes to the PM at 0 min (arrows) and to EE at 2 min in L2-sh3 and L2-sh4 cells as well as in L2-Luc controls. At 5 and 15 min, megalin accumulates at the ERC in L2-Luc cells (arrowheads) but remains scattered in peripheral vesicles in L2-sh3 and L2-sh4 cells (arrows). Coverslips were placed on ice to stop endocytosis followed by incubation with 20B mAb, which binds to cell surface megalin. Cells were either fixed directly (0 min) or incubated for 2, 5, or 15 min at 37°C to allow endocytosis and then fixed and incubated with Alexa Fluor 594 anti–mouse $F(ab')_2$ to detect megalin. (C) Megalin (red) colocalizes with the EE marker EEA1 (green) at 2 min in both L2-sh3 cells and L2-Luc controls. 20B mAb uptake was performed as in B. (D) At 15 min megalin (red) strongly colocalizes with Rab11 (green) in L2-Luc but not in L2-sh3 cells. 20B mAb uptake was performed as in B, and Rab11 was detected using Alexa Fluor 488–conjugated Rab11 mAb. (E) In L2-Luc controls TR-Tf (red) and megalin (green) colocalize at the ERC at 15 min. In L2-sh3 cells TR-Tf arrives at the ERC, but megalin fails to do so and remains in peripheral vesicles. Megalin colocalized with TfR at the ERC in 97.4 ± 0.8% of L2-Luc cells vs.15.9 ± 8.7% of the L2-sh3 cells (mean ± SEM, n = 3, 1,056 control cells and 823 ARH-depleted cells were counted). Cells were incubated with 20B mAb and TR-Tf on ice (30 min) and switched to 37°C (15 min) before fixation and processing for IF. Bar, 2.5 µm. Insets, 4×.

megalin traffic to the ERC (Fig. 2 B). Moreover, when ARH-His Y117D, a PTB domain mutant that perturbs ARH's interaction with megalin (Fig. S3), was delivered into L2-sh3 cells, it failed to restore trafficking of megalin to the ERC (Fig. 2 C). Adenoviral expression of human ARH (resistant to the rat ARH sh3 shRNA) in L2-sh3 cells also restored megalin trafficking to normal (Fig. S4). Taken together, these data suggest that ARH depletion or a mutant that interferes with ARH's interaction with megalin perturbs the sorting and/or delivery of megalin to the ERC.

Trafficking of megalin to the ERC is perturbed after depletion of ARH but not Dab-2

Dab-2 interacts with the second FXNPXY motif of megalin and has been suggested to be important for megalin endocytosis (Nagai et al., 2005) and to compensate for ARH deficiency during endocytosis (Keyel et al., 2006; Maurer and Cooper, 2006). To test the effect of Dab-2 knockdown on megalin trafficking, Dab-2 siRNA was delivered to L2-Luc and L2-sh3 cells by complexing it with PTD-DRBD, a protein-based siRNA delivery tool (Eguchi et al., 2009). A >90% reduction in Dab-2 levels was achieved (Fig. 3 B). In 20B uptake assays, equal surface labeling was observed in Dab-2–depleted cells and controls before warming (Fig. 3 A; 0 min). However, megalin internalization was markedly inhibited in Dab-2–depleted cells at 2 min as most of the megalin was still present at the cell surface, whereas in controls most of the megalin was in endosomes (Fig. 3 A). Moreover, in Dab-2–depleted cells much less megalin had arrived at the ERC by 5 min, but by 15 min there was no apparent difference from controls (Fig. 3 A). These results suggest that Dab-2 knockdown leads to delayed internalization of megalin from the PM, and, unlike ARH, Dab-2 does not have a significant role in trafficking of megalin after internalization. When Dab-2 was depleted in L2-sh3 cells, i.e., both ARH and Dab-2 were depleted, megalin failed to be internalized even after 5 min

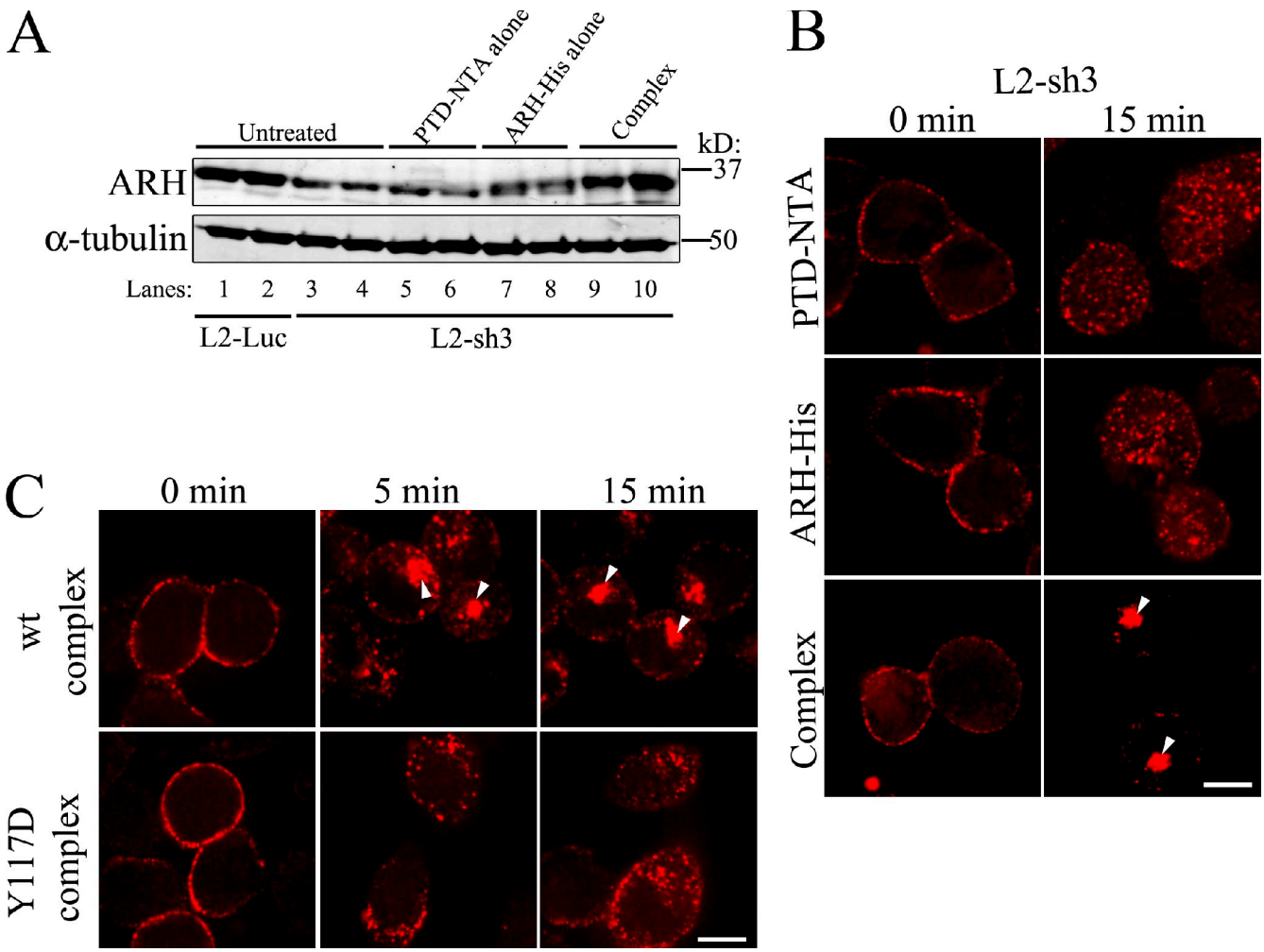

Figure 2. **Delivery of wtARH-His protein to ARH knockdown cells restores trafficking of megalin to the ERC.** (A) ARH levels in L2-sh3 cells are restored to approximately control levels by intracellular delivery of wtARH-His. L2-sh3 cells were incubated with PTD-NTA alone (lanes 5 and 6) or 1 µM wtARH-His alone (lanes 7 and 8), or a complex of ARH-His: PTD-NTA (lanes 9 and 10) for 90 min, lysed and immunoblotted for ARH and α-tubulin. Lanes 1 and 2: Lysates from untreated L2-Luc cells. Lanes 3 and 4: Lysates from untreated L2-sh3 cells. (B) Megalin (red) trafficking to the ERC is restored at 15 min (arrowheads) in cells treated with ARH-His–PTD-NTA (Complex) but not in cells treated with PTD-NTA or ARH-His alone. L2-sh3 cells were either treated with PTD-NTA alone, ARH-His alone, or a complex of ARH-His–PTD-NTA as described in A, followed by 20B mAb uptake. (C) Trafficking of megalin to the ERC (arrowheads) is restored after intracellular delivery of wtARH-His (wt complex) but not ARH-His Y117D (Y117D complex). wtARH-His and ARH-His Y117D were delivered into L2-sh3 cells as in A, and trafficking of megalin followed as in B. Bar, 2.5 µm.

(Fig. 3 A), indicating that ARH may be partly responsible for mediating the internalization of megalin in the absence of Dab-2. Additionally, depletion of both these PTB domain proteins led to diffuse distribution of megalin at the PM unlike controls, which show a punctate PM distribution, indicating a failure of sorting into clathrin-coated pits. Taken together, our data suggest that the primary role of Dab-2 is to facilitate internalization of megalin from the PM, whereas ARH determines the receptor's post-internalization fate. In the absence of Dab-2, ARH can partially facilitate the internalization of megalin.

ARH couples megalin to dynein

We previously reported that ARH interacts with dynein intermediate chain (DIC) and dynein heavy chain (DHC) subunits of the dynein motor complex (Lehtonen et al., 2008), which facilitates transport of cargo along microtubules toward the center of the cell including that to the ERC (Palmer et al., 2009). We reasoned that because ARH depletion leads to a defect in trafficking of megalin from EE to the ERC, ARH may be involved in facilitating trafficking of vesicles containing megalin to the ERC. To investigate this possibility we used MDCK-M4-ARH cells that stably overexpress FLAG-ARH and HA-M4, an HA-tagged megalin mini-receptor. We have previously shown that FLAG-ARH interacts with HA-M4 in these cells (Nagai et al., 2003). MDCK-M4-ARH cells were transiently transfected with myc-tagged DIC (myc-IC2), and immunoprecipitation (IP) was performed with anti-HA IgG. Both FLAG-ARH and myc-IC2 coimmunoprecipitated with HA-M4 (Fig. 4 A, lane 3). To test whether interaction between megalin and dynein is through ARH, the immunoprecipitates were incubated with two peptides containing megalin's first FXNPXY motif. Both peptides perturbed the interaction of megalin with ARH as well as with dynein (Fig. 4 A, lanes 7–12) whereas a control peptide had no effect (Fig. 4 A, lanes 4–6), suggesting that megalin's

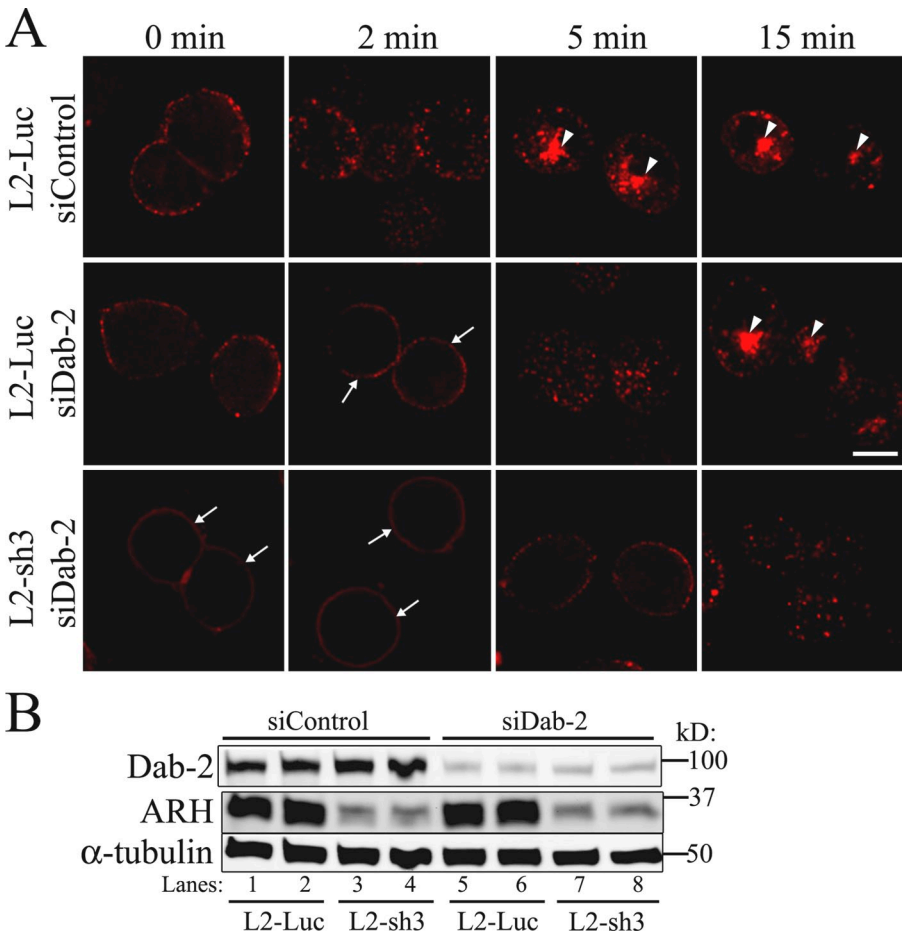

Figure 3. **Dab-2 knockdown delays internalization of megalin but does not affect its post-endocytic trafficking.** (A) At 2 min megalin is internalized into EE in control cells (siControl), whereas after Dab-2 depletion (siDab-2) a significant amount of megalin remains at the PM (arrows), indicating that megalin trafficking from the PM to EE is delayed. At 15 min, accumulation of megalin at the ERC is seen in Dab-2–depleted cells (arrowheads), and there is little, if any, difference in megalin distribution from controls. After depletion of Dab-2 in ARH-depleted L2-sh3 cells, megalin is diffusely distributed at the PM at 0 and 2 min (arrows) and is not internalized up to 5 min. Megalin internalization is observed at 15 min (i.e., significantly later than in controls or after Dab-2 depletion alone). L2-Luc and L2-sh3 cells were treated with PTD-DRBD–siRNA complex; 48 h after siRNA delivery, trafficking of megalin was followed using 20B mAb as described for Fig. 1 B. Bar, 2.5 µm. (B) L2 cells treated with Dab-2 siRNA (siDab-2; lanes 5–8) show 90% reduction in Dab-2 compared with cells treated with a control siRNA (siControl; lanes 1–4).

interaction with dynein is dependent on its ability to interact with ARH. Consistent with this conclusion, GST-megalin tail (GST-MT) interacted with endogenous dynein and ARH from lysates prepared from wt mouse embryonic fibroblasts (MEFs) but not from ARH$^{-/-}$ MEFs (Fig. 4 B, lanes 5 and 6). To further verify that the interaction between the first FXNPXY motif of megalin and ARH is necessary for megalin's interaction with dynein, we mutated Y81, the key tyrosine within this motif, to cysteine (Y81C). A homologous Tyr-to-Cys mutation (Y807C) within the FXNPXY motif of LDLR (the JD mutation) markedly reduces interaction between the LDLR and the PTB domain of ARH and leads to hypercholesterolemia (Davis et al., 1986; Dvir et al., 2012). As predicted, GST-MT Y81C markedly reduced interaction with ARH as well as with dynein (Fig. 4 C, lane 4), whereas a similar mutation in the second FXNPXY motif (which perturbs megalin binding to Dab-2) did not (Fig. 4 C, lane 5). We conclude that the interaction of megalin with dynein is dependent on the ability of its first FXNPXY motif to bind ARH, suggesting that ARH may serve to recruit dynein to megalin-containing vesicles and facilitate their trafficking to the ERC.

ARH knockdown leads to fast recycling of megalin via a Rab35 pathway

To investigate the fate of megalin after ARH depletion, we followed megalin's itinerary over time. In L2-Luc cells, as in wt L2 cells (Nagai et al., 2003), megalin trafficked to the ERC by 15 min and recycled back to the PM by 60 min (Fig. 5 A). In contrast, in L2-sh3 and L2-sh4 cells megalin arrived at the PM significantly faster (30 min) than in L2-Luc controls (Fig. 5 A). To verify and extend the immunofluorescence (IF) results we performed biotinylation assays on L2-Luc and L2-sh3 cells expressing M4-GFP. We selectively biotinylated receptors present at the cell surface and followed their internalization and recycling. To measure the amount of M4-GFP and TfR present at the cell surface, cells were lysed immediately after biotinylation, and the biotinylated receptors were isolated and analyzed by immunoblotting. The amounts of M4-GFP and TfR at the cell surface were comparable in L2-Luc and L2-sh3 cells (Fig. 5 B, lane 2). To measure internalization, cells were treated with lactoferrin, a megalin ligand, and transferrin for 10 min, followed by treatment with 2-mercaptoethanesulfonic acid (MESNA), which cleaves biotin from proteins at the PM, allowing selective isolation of internalized biotinylated receptors. In both L2-Luc and L2-sh3 cells, virtually all the M4-GFP at the surface was internalized within 10 min (Fig. 5 B, lane 4). To measure recycling, cells were incubated at 37°C to allow the internalized biotinylated receptors to recycle to the PM and again treated with MESNA. In L2-Luc cells, recycling of M4-GFP (indicated by the reduction in the intracellular pool of biotinylated receptor) was not detected until 55 min (Fig. 5 B, lane 7), whereas in L2-sh3 cells recycling of M4-GFP to the cell

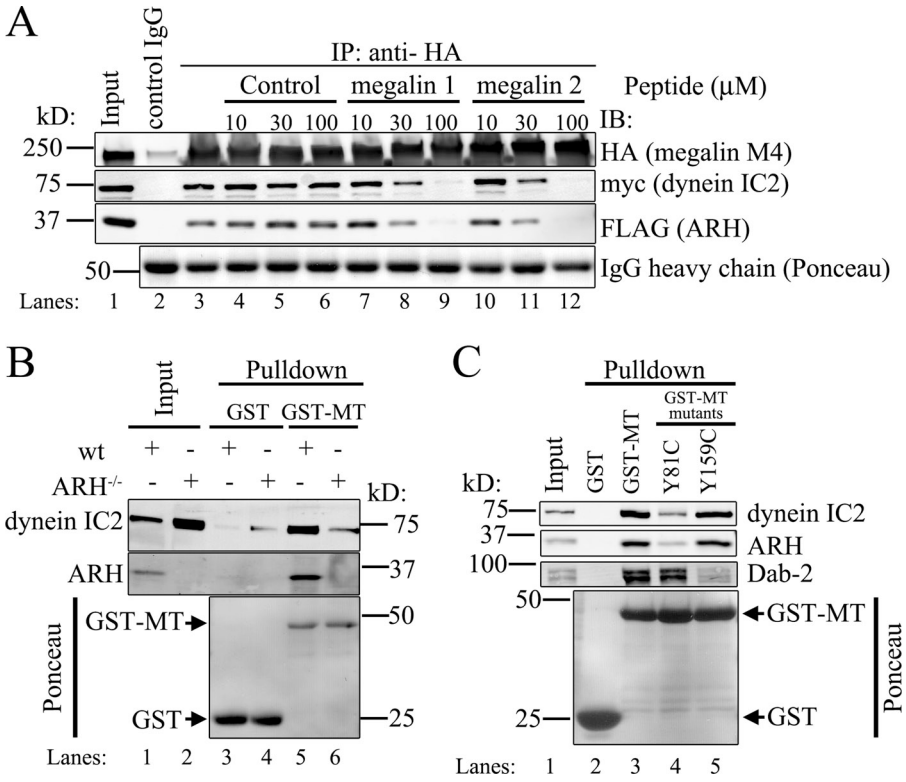

Figure 4. **ARH mediates the interaction between megalin and dynein.** (A) myc-dynein IC2 and FLAG-ARH coimmunoprecipitate with HA-tagged mini-megalin (megalin-M4). Incubation of the immunoprecipitates with peptides (megalin 1, 2) spanning megalin's first FXNPXY motif (which binds ARH) reduces interaction of megalin with both FLAG-ARH and myc-dynein IC2, indicating that binding of dynein to megalin depends on the interaction between ARH and megalin. MDCK-M4-ARH cells were transiently transfected with myc-dynein IC2, and IP was performed with anti-HA mAb (lanes 3–12) or control IgG (lane 2) followed by immunoblotting for HA, myc, or FLAG. Immunoprecipitates were treated with 10, 30, or 100 μM megalin (lanes 7–9 and 10–12) or control (lanes 4–6) peptides. Lane 1: 5% of the starting material used for the IP (Input). (B) Pull-down assay showing that GST-MT binds dynein IC2 from wt MEFs (lane 5), but binding is significantly reduced in ARH$^{-/-}$ MEFs (lane 6). GST or GST-MT was incubated with lysates from wt or ARH$^{-/-}$ MEFs, and bound dynein IC2 and ARH were analyzed by immunoblotting. Lanes 1 and 2: 5% of the wt and ARH$^{-/-}$ MEF lysates used for pull-down (Input). Bottom panel: Ponceau S staining to visualize GST proteins. (C) A mutation (Y81C) in the first FXNPXY motif of megalin tail, which binds ARH, reduced its interaction with both ARH and dynein IC2. However, a mutation (Y159C) in the second FXNPXY motif of megalin, which binds Dab-2, did not affect the interaction with dynein IC2. Pull-down assays were performed on wt MEF lysates using GST (lane 2), GST-MT (lane 3), GST-MT Y81C (lane 4), or GST-MT Y159C as in B. Bottom panel: Ponceau S staining to visualize amount of GST proteins.

surface was faster and was detected as early as 25 min (Fig. 5 B, lane 5). Nearly 60% of the M4-GFP had returned to the PM in L2-sh3 cells by 25 min, whereas in controls only 3% had returned (Fig. 5 C). The apparent increase in intracellular levels of megalin in L2-sh3 cells at 40 min is most likely due to internalization of the megalin that had recycled to the PM by 25 min. As expected, ARH knockdown did not alter the recycling kinetics of TfR (Fig. 5 B). Thus, the biotinylation data confirm that ARH knockdown leads to faster recycling of megalin, suggesting that in the absence of ARH megalin takes the fast recycling pathway directly from EE.

Rab35 GTPase associates with vesicles that traffic from EE to the PM and regulates the fast recycling of receptors that follow this route (Kouranti et al., 2006). Rab35, like other Rab family members, cycles between its active GTP-bound form that is membrane associated and the inactive GDP form that is predominantly cytosolic (Pfeffer and Aivazian 2004, Goody et al., 2005, Egami et al., 2011). To determine whether megalin recycles through this pathway in ARH knockdown cells we localized megalin and Rab35 by IF. In L2-Luc cells most of the megalin localized to the ERC at 15 min, and Rab35 was diffusely distributed in the cytoplasm (Fig. 5 D). In contrast, in the ARH-depleted L2-sh3 cells most of the megalin colocalized with Rab35 on EE at 15 min (Fig. 5 D), confirming that megalin takes the fast recycling pathway after ARH depletion. Our finding that Rab35 shifts from a cytosolic distribution in controls to endosomal membranes after ARH knockdown is an indirect indicator that Rab35 becomes activated after ARH knockdown. Additionally, Rab35 was markedly increased in membrane fractions (100,000 *g* pellet) from L2-sh3 cells compared with L2-Luc controls (Fig. 5 E), thus verifying the increased membrane association of Rab35 and its presumed activation after ARH depletion.

ARH binding to AP-2 is necessary to prevent fast recycling of megalin

We noted that connecdenn2 (also known as DENN1B), a guanine nucleotide exchange factor (GEF) for Rab35 (Allaire et al., 2010), binds to the same site on AP-2 (the β2 appendage) as ARH, and ARH and connecdenn2 compete for binding to this site in vitro (Marat and McPherson, 2010). Thus, we reasoned that (1) ARH might normally prevent the fast recycling of megalin by binding to AP-2 and preventing binding of connecdenn2, and (2) in the absence of ARH connecdenn2 might bind AP-2 vesicles containing megalin, activate Rab35, and stimulate rapid recycling of megalin. To find out whether connecdenn2 is involved in the fast recycling of megalin, we knocked down connecdenn2 (Fig. 6 B). Connecdenn2 depletion had no visible effect on megalin trafficking through the ERC in L2-Luc cells (not depicted). In contrast, in L2-sh3, which normally show fast

recycling of megalin, no recycling of megalin was detected at 30 min after connecdenn2 depletion (Fig. 6 A). Instead, at 30 min, megalin localized in large, clustered endosomes (Fig. 6 A), suggesting that after connecdenn2 knockdown megalin is internalized and reaches EE, but cargo fails to exit EE, leading to their enlargement and clustering. The enlargement and clustering of EE after connecdenn2 depletion is consistent with previous observations (Allaire et al., 2010). These results suggest that after ARH depletion fast recycling of megalin is mediated by connecdenn2.

To test whether interaction of ARH with AP-2 is necessary to prevent megalin from taking the fast recycling pathway we used ARH R265A, an ARH mutant defective in AP-2 binding (He et al., 2002; Mishra et al., 2002). wtARH-His or ARH-His R265A delivered into L2-sh3 cells returned ARH expression to endogenous levels (Fig. 6 E). As expected, delivery of wtARH-His to L2-sh3 cells fully restored megalin trafficking to the ERC at 15 and 30 min, and no recycling to the PM was seen at 30 min (Fig. 6 C). In contrast, when the mutant ARH-His R265A was delivered a pool of megalin colocalized with Rab35 at 15 min (Fig. 6 D) and arrived at the PM by 30 min (Fig. 6 C), indicating that the mutant was not able to fully restore megalin trafficking to the ERC. We conclude that ARH binding to AP-2 is necessary for the efficient trafficking of megalin to the ERC. Similar results were obtained when wt ARH or an AP-2–binding deficient ARH mutant was adenovirally expressed in L2-sh3 cells (Fig. S5). The finding that a pool of megalin was able to traffic to the ERC in the presence of ARH-His R265A may be due to the fact that this mutation does not perturb the ability of ARH to interact with dynein (Fig. S5). From these data we conclude that binding of ARH to AP-2 is necessary to prevent fast recycling of megalin via the connecdenn2–Rab35 pathway.

Taken together, our results indicate that ARH utilizes two distinct mechanisms to regulate megalin's endocytic trafficking: (1) it couples megalin to dynein and facilitates its trafficking from EE to the ERC, and (2) it binds AP-2 and inhibits fast recycling of megalin from EE.

ARH regulates intramembrane proteolysis and gene expression of megalin

Next we investigated the functional consequences of megalin's trafficking through the ERC. Megalin, like many other receptors, undergoes RIP in two steps: (1) the ectodomain is cleaved generating a 35–40-kD cytoplasmic tail fragment (MCTF), and (2) MCTF is cleaved within the transmembrane domain by γ-secretase to generate a 25–30-kD soluble megalin intracellular domain (MICD; Zou et al., 2004; Li et al., 2008). Because RIP of many receptors occurs along the endocytic pathway (De Strooper and Annaert 2010) we reasoned that ARH-mediated trafficking of megalin to the ERC might be required for proteolytic processing of megalin. To investigate this possibility, we checked for the presence of megalin fragments in ARH-depleted cells using an antibody that specifically recognizes the cytoplasmic tail of megalin. ARH knockdown cells showed a greater than twofold increase in a ∼37-kD fragment, the expected size of MCTF (Fig. 7 A), indicating a marked accumulation of MCTF after ARH depletion. No band corresponding to MICD was visible, a finding consistent with previous results, indicating that cleaved fragments of receptors produced by RIP are rapidly degraded by proteasomes (Kopan and Ilagan 2004). To detect MICD, we treated L2-Luc and L2-sh3 cells with 2–10 µM lactacystin, a proteasome inhibitor. L2-Luc cells treated with lactacystin showed a dose-dependent accumulation of a 28-kD peptide, the expected size of MICD, as well as a number of intermediate fragments (Fig. 7 B, lanes 3–5). In sharp contrast, very little MICD was detected in L2-sh3 cells even after 10 µM lactacystin treatment (Fig. 7 B, lanes 6–8). These data suggest that MCTF accumulates after ARH depletion due to decreased γ-secretase–mediated proteolysis of megalin. We conclude that ARH-mediated trafficking of megalin from EE to the ERC is necessary for γ-secretase–mediated RIP of megalin.

MICD and the cleaved intracellular domains of many receptors that undergo RIP translocate to the nucleus and transcriptionally regulate gene expression (Li et al., 2008; De Strooper and Annaert 2010). In the case of megalin, MICD has been shown to repress expression of megalin as well as the Na^+-H^+ exchanger 3 (NHE3), another membrane protein present at the brush border of the proximal tubule (Li et al., 2008). Because ARH-depleted cells show reduced MICD levels, we tested whether there was a change in megalin expression and found that L2-sh3 and L2-sh4 cells showed a 2.2- and 1.9-fold increase, respectively, in levels of full-length megalin (Fig. 7 A). To verify that increased megalin is due to increased transcription, we performed RT-PCR analysis of mRNA isolated from L2-Luc and L2-sh3 cells. L2-sh3 cells showed a 2.7-fold increase in megalin mRNA with no significant change in expression of a control gene, GAPDH (Fig. 7 C). Expression of NHE3 mRNA in L2-sh3 cells was also increased 3.4-fold (Fig. 7 C). These data establish that the increased levels of full-length megalin observed in ARH knockdown cells is associated with increased mRNA expression. We conclude that ARH depletion reduces the RIP of megalin and thus the formation of MICD fragments, which leads to increased transcription of megalin and NHE3. Our data thus imply that ARH-mediated trafficking of megalin to the ERC is necessary for it to undergo RIP and to regulate its expression.

Discussion

Here we report that ARH is required for megalin trafficking to the ERC. Based on our findings, we propose the following model (Fig. 8 A): The megalin–ARH–AP2 complex is taken up by clathrin-mediated endocytosis and delivered to EE, where ARH recruits dynein and facilitates vesicular transport of megalin along microtubules toward the ERC. Megalin recycles from the ERC back to the PM via the slow recycling pathway. In the absence of ARH, connecdenn2 binds AP-2 and associates with megalin endosomes, activates Rab35, and mediates fast recycling of megalin-containing vesicles to the PM directly from EE. A small amount of megalin undergoes ectodomain cleavage at the PM producing MCTF (Fig. 8 B). Like full-length megalin, MCTF is internalized by endocytosis and then traffics to the ERC. At the ERC, MCTF is cleaved by γ-secretase to release MICD, which translocates to the nucleus and regulates gene

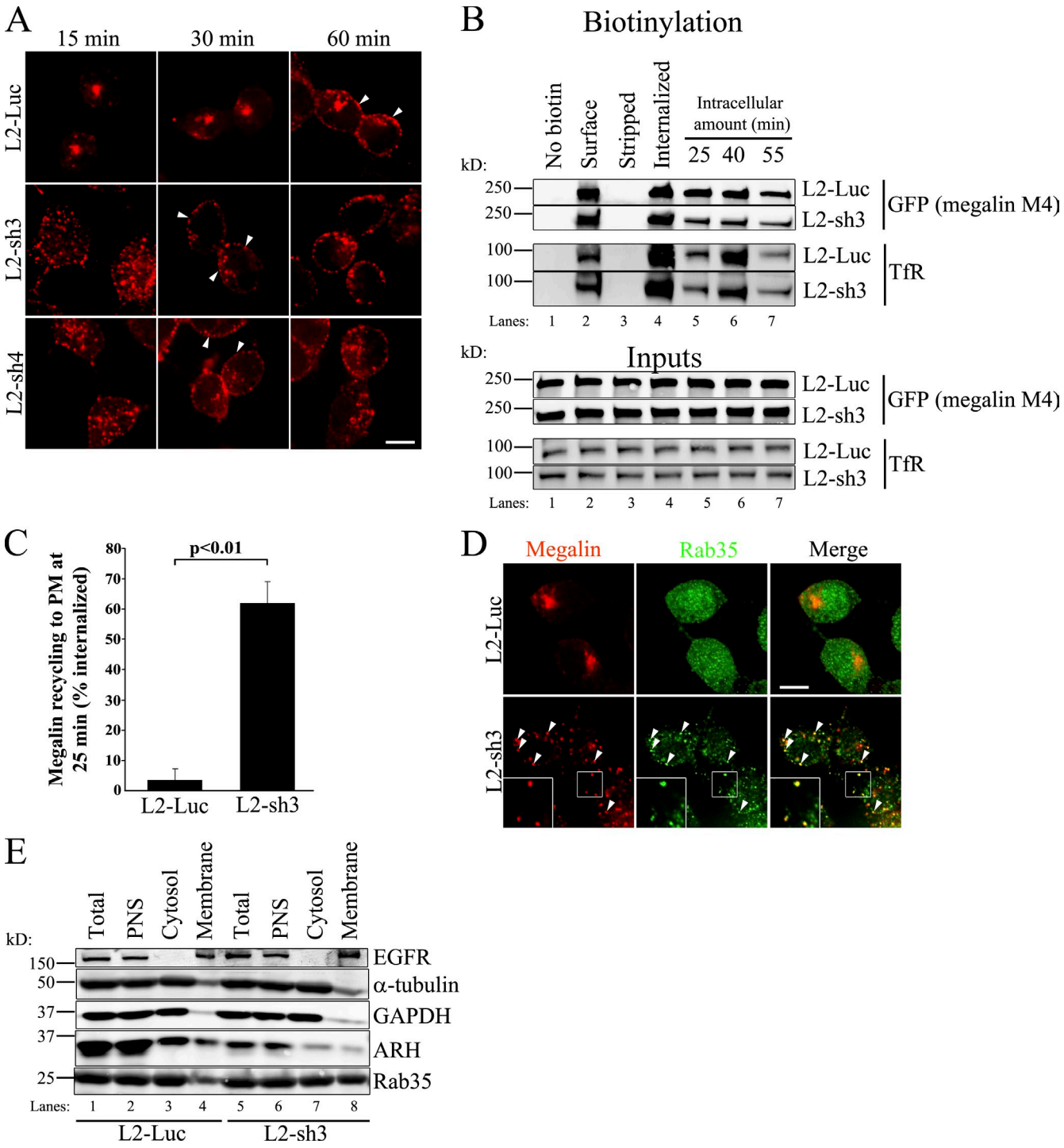

Figure 5. **ARH knockdown leads to fast recycling of megalin to the PM.** (A) In control L2-Luc cells megalin accumulates at the ERC at 15 and 30 min and returns to the PM by 60 min (arrowheads). In contrast, in L2-sh3 and L2-sh4 cells megalin does not accumulate at the ERC and recycles to the PM by 30 min (arrowheads). 20B mAb binding and internalization were performed as described in Fig. 1 B. (B) Biotinylation assay to assess the effect of ARH depletion on megalin recycling. Top: biotinylated proteins isolated on a NeutrAvidin column. Bottom: total receptors in the corresponding cell lysates. L2-Luc and L2-sh3 cells expressing M4-GFP mini-megalin were biotinylated, and the biotinylated cell surface proteins were isolated and immunoblotted for GFP or TfR. Lane 1: little or no M4-GFP or TfR is detectable in the absence of biotin, indicating minimal background binding of nonbiotinylated receptors to the NeutrAvidin column. Lane 2: the amounts of M4-GFP and TfR at the cell surface (Surface) are comparable in L2-Luc and L2-sh3 cells. Lane 3: when biotinylation of cell surface receptors is followed immediately by MESNA treatment (Stripped), little M4-GFP or TfR is detectable, indicating that MESNA efficiently cleaves biotin from surface receptors. Lane 4: to measure internalization of M4-GFP after biotinylation, cells were incubated at 37°C for 10 min in the presence of lactoferrin and transferrin and then treated with MESNA. The amount of M4-GFP and TfR internalized at 10 min is nearly equal in L2-Luc and L2-sh3 cells. Lanes 5–7: to measure recycling of M4-GFP and TfR, cells were then switched to 37°C for an additional 25, 40, or 55 min to resume endocytic trafficking/recycling of the internalized biotinylated receptors and then treated again with MESNA to cleave the biotin from receptors that had recycled to the PM. In L2-Luc cells the reduction in intracellular M4-GFP (a measure of receptor recycling) is noticeable at 55 min, indicative of slow recycling of megalin in these cells compared with L2-sh3 cells in which a reduction in M4-GFP is visible by 25 min, indicative of fast recycling. No significant

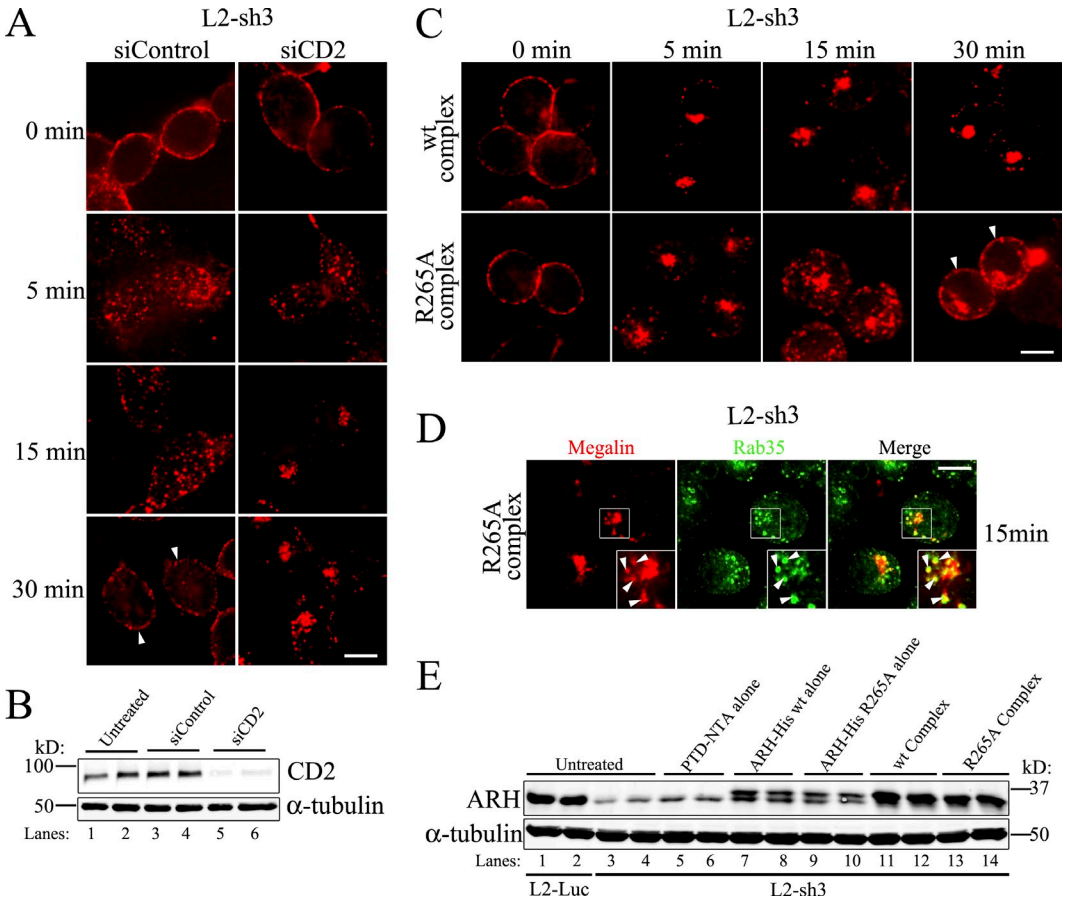

Figure 6. **Binding of ARH to AP-2 prevents fast recycling of megalin through the connecdenn2–Rab35 pathway.** (A) In L2-sh3 ARH-depleted cells treated with control siRNA (siControl), megalin is internalized into endocytic vesicles at 5 and 15 min and recycles back to the PM by 30 min (arrowheads), whereas in those treated with connecdenn2 siRNA (siCD2) there is little or no recycling at 30 min. siRNA knockdown of connecdenn2 was performed as for Fig. 3 B, and 48 h later megalin trafficking was analyzed as in Fig. 1 B. (B) L2-sh3 cells treated with connecdenn2 siRNA (siCD2; lanes 5 and 6) show >90% knockdown of connecdenn2 compared with control (siControl; lanes 3 and 4) or untreated L2-sh3 cells (lanes 1 and 2). siRNA delivery was performed as in Fig. 3 B. Each condition was tested in duplicate. (C) Delivery of wtARH-His (wt complex) into L2-sh3 cells restores megalin trafficking to the ERC by 5 min and prevents fast recycling to the PM at 30 min. In contrast, delivery of ARH-His R265A into L2-sh3 cells (R265A complex) led to fast recycling at 30 min (arrowheads) along with partial trafficking of megalin to the ERC. wtARH-His or ARH-His R265A protein was delivered to L2-sh3 cells using the PTD-NTA method as in Fig. 2 A, and trafficking of megalin was studied as in Fig. 1 B. (D) In L2-sh3 cells treated with ARH-His R265A, megalin colocalizes with the fast recycling marker Rab35 (green) in vesicles at 15 min (arrowheads). (E) wtARH-His (lanes 11 and 12) or ARH-His R265A (lanes 13 and 14) delivered into L2-sh3 cells restores ARH levels to near endogenous levels. Lysates from untreated L2-Luc (lanes 1 and 2) or L2-sh3 (lanes 3 and 4) cells, or from cells treated with PTD-NTA (lanes 5 and 6) or either protein alone (lanes 7–10) are also included.

expression. In the absence of ARH, MCTF cannot traffic to the ERC and hence cannot be processed into MICD.

Recycling of receptors (e.g., TfR) through the ERC has been known for over two decades (Maxfield and McGraw 2004), yet the physiological significance of recycling through the ERC versus EE has remained elusive. Several proteins that mediate general trafficking of cargo between EE and ERC (e.g., Rab10, SNX4) have been identified (Grant and Donaldson 2009), but no motifs responsible for sorting receptors from EE for delivery to the ERC have been reported to date. ARH, which interacts with the first FXNPXY motif of megalin, represents the first known protein that mediates the trafficking of a receptor to the ERC by engaging a specific sequence motif within the receptor and enabling it to bypass the fast recycling

differences in TfR endocytosis was seen among these cell lines. (C) Recycling of biotinylated M4-GFP in L2-Luc (61.6 ± 7%) and L2-sh3 cells (3.3 ± 3.6%) at 25 min expressed as a percentage of the amount internalized (mean ± SEM, $n = 3$ for each condition). (D) In L2-Luc cells megalin (red) accumulates at the ERC at 15 min and does not colocalize with Rab35 (green). By contrast, in L2-sh3 cells, megalin remains in scattered vesicles where it colocalizes with Rab35 (arrowheads), indicating fast recycling. 20B mAb uptake was performed in L2-Luc and L2-sh3 cells as for Fig. 1 B. Bar, 2.5 µm. Insets, 4×. (E) Rab35 distribution shifts from the cytosolic fraction to the membrane fraction after ARH depletion, indicative of increased Rab35 activation. In L2-Luc cells 78.3 ± 8.9% of the Rab35 is in the cytosolic fraction (lane 3), and 24.2 ± 6.1% is in the membrane fraction (lane 4). In L2-sh3 cells, 54.2 ± 7.6% Rab35 is in the membrane fraction (lane 8) vs. 49.4 ± 7.7% in the cytosolic fraction (lane 3; mean ± SEM, $n = 3$, expressed as percentage of Rab35 in the postnuclear supernatant "PNS" [lanes 2 and 6]). As expected, EGF receptor (EGFR) is found almost exclusively in the membrane fraction (lanes 4 and 8) and GAPDH and α-tubulin are predominantly in the cytosolic fraction (lanes 3 and 7). Cytosolic (100,000 *g* supernatant) and membrane (100,000 *g*) fractions prepared from L2-Luc and L2-sh3 cells were immunoblotted for the indicated proteins.

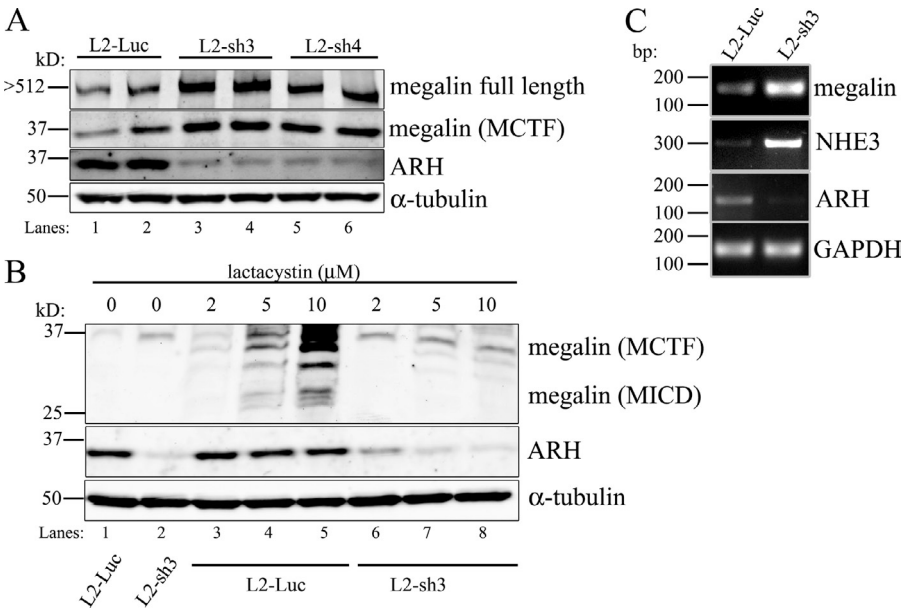

Figure 7. **ARH depletion leads to reduced intramembrane proteolysis of megalin and increased transcription of megalin and NHE3.** (A) The levels of megalin cytoplasmic tail fragment are increased 2.6 ± 0.4 and 2.3 ± 0.3-fold in L2-sh3 and L2-sh4 cells (mean ± SEM, $n = 3$) vs. L2-Luc controls, and full-length megalin levels are increased 2.2 ± 0.4 and 1.9 ± 0.3-fold (mean ± SEM, $n = 4$). Lysates were immunoblotted with antibody for ARH, α-tubulin, full-length megalin (LBDIV), and megalin tail fragments (459). (B) Levels of the megalin intracellular domain (MICD) fragment are reduced in ARH-depleted cells. L2-Luc and L2-sh3 cells were treated overnight with 2, 5, or 10 μM lactacystin to prevent proteasomal degradation of MICD. Cell lysates were immunoblotted as in A. MICD levels increase in a dose-dependent manner after lactacystin treatment of L2-Luc controls (lanes 3–5), whereas L2-sh3 cells show little or no accumulation of MICD with up to 10 μM lactacystin treatment (lanes 6–8). (C) RT-PCR showing that megalin and NHE3 mRNA levels are increased ∼2.7± 0.7 and 3.4 ± 0.9-fold, respectively, in L2-sh3 cells vs. L2-Luc cells (mean ± SEM, $n = 4$). No significant change is seen in GAPDH mRNA.

pathway. Moreover, our results showing that ARH-mediated megalin trafficking to the ERC is necessary for γ-secretase–mediated cleavage of megalin have revealed a new function for the ERC as a site for RIP.

Distinct functions of ARH and Dab-2: ARH is required for megalin trafficking from EE to the ERC, whereas Dab-2 mediates megalin internalization

The cytoplasmic tail of LDLR has only one FXNPXY, which can engage either ARH or Dab-2 to sort LDLR into clathrin-coated pits (Keyel et al., 2006; Maurer and Cooper 2006). In the absence of ARH, Dab-2 can facilitate endocytosis of LDLR in some cell types such as fibroblasts, which has led to the notion that the functions of ARH and Dab-2 are redundant. Unlike LDLR, megalin has two FXNPXY motifs, of which the first binds to ARH (Nagai et al., 2003) and the second to Dab-2 (Oleinikov et al., 2000). We show here that in the case of megalin these two proteins have separate functions: ARH is essential for trafficking of megalin to the ERC, whereas the primary role of Dab-2 is in mediating megalin's internalization, in keeping with its traditional role as a CLASP and consistent with previous observations in Dab-$2^{-/-}$ mice (Nagai et al., 2005). Our finding that ARH depletion inhibits megalin trafficking to the ERC is a departure from ARH's recognized role as a CLASP involved primarily in receptor internalization. The difference between the functions of ARH and Dab-2 can most likely be explained by the differences in the proteins they interact with. Dab-2 interacts with myosin VI (Morris et al., 2002), the motor protein responsible for trafficking of vesicles through the cortical actin barrier, which is in keeping with the role of Dab-2 in receptor internalization and the steps immediately after it. ARH interacts with the motor protein dynein (Lehtonen et al., 2008), which facilitates trafficking of cargo along microtubules to the pericentriolar region (see following paragraph).

ARH couples megalin to dynein for trafficking of megalin along microtubules to the ERC

We previously discovered that ARH interacts with the heavy and intermediate chains of the dynein motor complex (Lehtonen et al., 2008). A single dynein (cytoplasmic dynein) is responsible for virtually all cargo trafficking toward the minus-end of microtubules including trafficking of cargo to the ERC (Traer et al., 2007; Palmer et al., 2009). We show here that ARH acts as a dynein adaptor that couples megalin to dynein, which explains how ARH facilitates the trafficking of megalin from EE to the ERC. ARH can now be added to the list of proteins that function as dynein adaptors that recruit the dynein–dynactin complex to different organelles such as the Golgi (βIII-spectrin and Bicaudal D), endoplasmic reticulum (Sec23), late endosomes (Rab7-interacting lysosomal protein or RILP), and ERC (SNX4 and KIBRA) and facilitate their transport along microtubules (Kardon and Vale 2009). ARH depletion affects the trafficking of megalin but not of TfR, which does not interact with ARH but which also couples to dynein (Traer et al., 2007; Palmer et al., 2009) and traffics along the same route from EE to the ERC. This indicates that ARH is likely to specifically sort receptors with FXNPXY motifs. Indeed, the ARH Y117D mutant, which does not interact with the FXNPXY motif of megalin, failed to sort megalin for trafficking to the ERC. Whether this newly identified function of ARH as a dynein adaptor also applies to other FXNPXY motif–containing proteins such as LDLR, LRP, and ROMK (Fang et al., 2009), with which ARH also interacts, remains to be tested.

ARH binds to AP-2 and prevents the fast recycling of megalin via the connecdenn2–Rab35 pathway

While receptor recycling was originally considered to be a default pathway (Maxfield and McGraw 2004), it is now recognized to

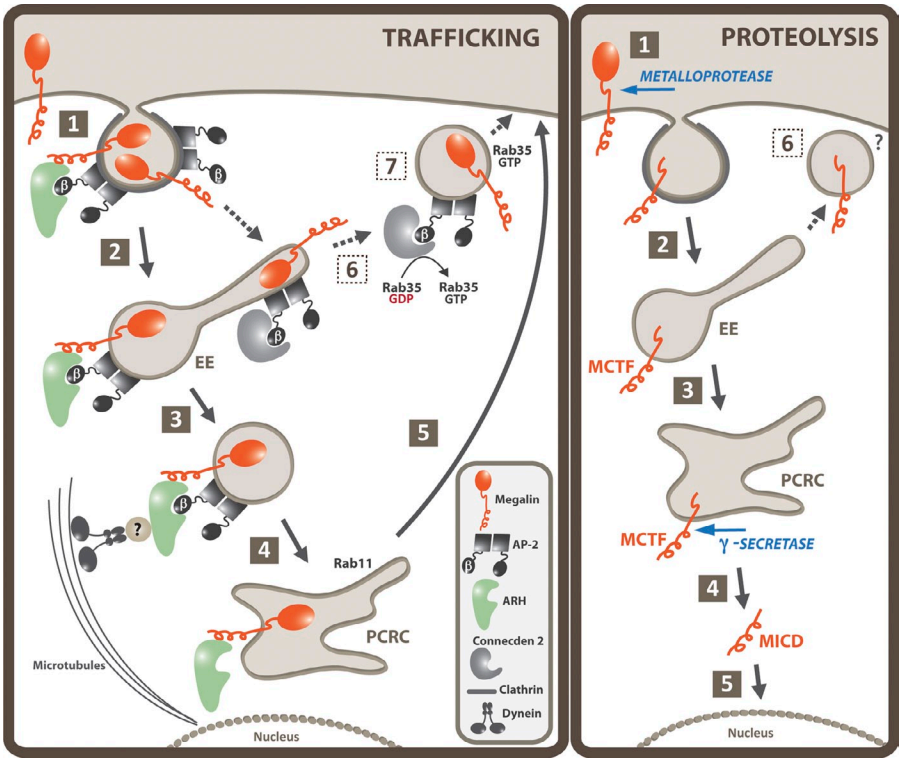

Figure 8. **Working model for the role of ARH in megalin trafficking and proteolysis.** (Left panel, 1) ARH binds to the cytoplasmic tail of megalin and to the β-appendage of AP-2. (2) The megalin–ARH complex is taken up in clathrin-coated vesicles and delivered to EE. (3) ARH recruits dynein to EE and (4) facilitates their transport along microtubules to the ERC, from where (5) megalin recycles back to the PM via the slow recycling pathway. In ARH-depleted cells (6) the β-appendage of AP-2 binds to connecdenn2 (CD2), which (7) activates Rab35 and directs the trafficking of megalin-containing vesicles to the PM via the fast recycling pathway. (Right panel) A fraction of the internalized megalin undergoes RIP. (1) The ectodomain of megalin is cleaved at the PM by a matrix metalloprotease to generate the MCTF fragment (Zou et al., 2004), which (2) is internalized into EE and, (3) like the full-length receptor, traffics to the ERC. (4) MCTF is cleaved at the ERC by γ-secretase to release the MICD fragment, which (5) translocates to the nucleus where it regulates gene expression. (6) In the absence of ARH, MCTF is not delivered to the ERC and hence is not processed by γ-secretase to yield MICD.

involve active sorting via sequence motifs within the cytoplasmic tails of receptors (Hanyaloglu and von Zastrow 2008; Hsu et al., 2012). However, no sequence motif involved in directing trafficking of receptors from EE to ERC has been identified up to now. Our results have revealed that ARH interacts with the first FXNPXY motif in the cytoplasmic tail of megalin and directs megalin away from the fast recycling pathway to the slow recycling pathway. Thus, our results suggest that active, sequence-based sorting is needed to direct cargo to the ERC for slow recycling back to the PM.

Our results suggest that fast recycling of megalin in ARH-depleted cells involves activation of the GTPase Rab35, the Rab that specifically mediates fast recycling of other receptors (Kouranti et al., 2006), and it also requires connecdenn2, a GEF that activates Rab35 (Allaire et al., 2010). Although other DENN domain–containing proteins (e.g., connecdenns 1 and 3) can also act as GEFs for Rab35, connecdenn2 is the only known member of the DENN domain family that interacts with the clathrin machinery, specifically clathrin and the β subunit of AP-2 (Marat and McPherson 2010). In fact, Both ARH and connecdenn2 bind to the same site on the β appendage of AP-2 (Marat and McPherson 2010). Based on our observation that binding of ARH to AP-2 is essential to prevent fast recycling of megalin, we postulate that ARH normally prevents megalin from taking the fast recycling pathway by competing with connecdenn2 for AP-2 binding (Fig. 8), preventing connecdenn2 from associating with megalin-containing endosomes and in turn preventing the activation of Rab35 on these endosomes. Interestingly, β-arrestins bind to the same site on the AP-2 β subunit as ARH and connecdenn2, suggesting that β-arrestins may also serve to regulate the recycling pathway taken by the G protein–coupled receptors to which they bind (Laporte et al., 2000; Traub 2009).

ARH-mediated trafficking of megalin to the ERC is necessary for regulating its proteolysis and gene expression

We show here that ARH-mediated trafficking to the ERC is required for RIP of megalin, which releases MICD and regulates gene expression. ARH depletion results in reduced levels of MICD and increased levels of MCTF, most likely due to reduced γ-secretase–mediated cleavage of MCTF, which is required to release MICD. The idea that the ERC may be a site for γ-secretase–mediated proteolysis during RIP is supported by two additional observations: (1) presenilin1, the catalytic subunit of γ-secretase, has been reported to interact with Rab11, the GTPase associated with ERC (Dumanchin et al., 1999), and (2) inhibition of γ-secretase activity resulted in accumulation of the cytoplasmic tail fragments of APP (Zhang et al., 2006) and megalin (Li et al., 2008) in the ERC. Our results indicating that ARH-mediated megalin trafficking to the ERC is essential for its RIP provide direct evidence that this is the case. Interestingly, TfR, the best-studied receptor that traffics to the ERC, is cleaved by a matrix metalloprotease and undergoes ectodomain shedding (Kaup et al., 2002), and the levels of the shed TfR ectodomain in human serum strongly correlate with elevated levels of erythropoietic activity and TfR expression (Skikne et al., 1990). Whether TfR also undergoes classical RIP at the ERC remains to be established.

It was previously shown that MICD, the final product of γ-secretase–mediated RIP of megalin, translocates to the nucleus and regulates gene expression (Li et al., 2008), as is the case with some other receptors (De Strooper and Annaert 2010), and overexpression of MICD led to suppression of megalin and NHE3 expression (Li et al., 2008). Consistent with these findings, we observed increased mRNA levels of megalin and NHE3

after ARH depletion, indicating that ARH-facilitated trafficking of megalin through the ERC is important for the regulation of gene expression mediated by megalin fragments.

Disease implications of ARH's role in megalin trafficking and proteolysis

Megalin mediates the uptake of a large number of ligands in different tissues including the kidney, lungs, yolk sac, thyroid, and parathyroid (Christensen and Birn 2002). The best studied function of megalin is the retrieval of albumin and low molecular weight proteins such as vitamin D–binding protein from the glomerular filtrate in the renal proximal tubule (Christensen and Birn 2002). Our findings that ARH-mediated trafficking of megalin to the ERC results in RIP of megalin and inhibition of megalin and NHE3 gene expression suggest the existence of a negative feedback loop for regulation of the expression of megalin and related kidney proteins. This pathway may allow the cell to adjust to changes in the ligand load during normal and pathological conditions. For example, under conditions of increased glomerular permeability, which lead to increased ligand load, megalin might be rerouted through the fast recycling pathway via unknown mechanisms, reducing its RIP and increasing its expression.

In summary, our study has revealed a surprising role for ARH in regulating the trafficking of megalin, its proteolysis, and gene expression via new molecular mechanisms. This paradigm may be applicable to other proteins such as LDLR, LRP, and ROMK, with which ARH interacts.

Materials and methods

Materials

Primers were ordered from Allele Biotech, restriction enzymes and reagents for polymerase chain reaction (PCR) were from New England Biolabs, Inc., except for PfuUltra DNA polymerase, which was from Agilent Technologies. Chemical reagents were obtained from Sigma-Aldrich except where noted. All cell culture reagents including DMEM, fetal bovine serum, penicillin, streptomycin, L-glutamine, Dulbecco's phosphate-buffered saline (PBS), and 0.05% trypsin-EDTA were purchased from Invitrogen.

Cell culture

L2 rat yolk sac cells (Orlando and Farquhar 1993) were maintained in DMEM Hi-glucose, supplemented with 10% fetal calf serum and 100 U/ml penicillin G and 100 µg/ml streptomycin sulfate (Invitrogen) at 37°C and 5% CO_2. MDCK-M4-ARH cells that stably express a megalin mini-receptor (HA-M4) and FLAG-ARH were prepared and maintained as described previously (Nagai et al., 2003). Wild-type and $ARH^{-/-}$ MEFs and HEK 293T cells were cultured as described previously (Lehtonen et al., 2008).

Antibodies

Polyclonal rabbit anti-megalin antibodies against the ectodomain (LBD IV) and cytoplasmic tail (459) of megalin (Czekay et al., 1995) and polyclonal rabbit anti-ARH raised against GST-ARH 177–299 (Nagai et al., 2003) were described previously. A mouse anti-megalin mAb 20B against the ectodomain of megalin (Miettinen et al., 1990) was produced from hybridoma cells cultured in a CELLine-1000 bioreactor (Sartorius Stedim) according to the manufacturer's protocol using Hybridoma-SFM medium (Invitrogen). Hybridoma media was collected, cleared by centrifugation (20,000 *g* for 30 min), its purity (95%) was verified by SDS-PAGE, and a fresh aliquot was used for each 20B uptake assay. Anti-transferrin receptor (H68.4) mAb was from Ian Trowbridge (formerly of Salk Institute, San Diego, CA), anti-Rab11 mAb from BD, and anti-FLAG (M2) and anti-tubulin mAbs from Sigma-Aldrich. Rabbit Rab35 pAb was from Bruno Goud (Institut Curie, Paris, France), EEA1 from Cell Signaling Technology, and connecdenn2 from Peter McPherson (McGill University, Montreal, Canada). Cross-absorbed Alexa 488–conjugated goat anti–rabbit and Alexa 594–conjugated goat anti–mouse $F(ab')_2$ for indirect IF were purchased from Molecular Probes. Goat anti–rabbit and goat anti–mouse Alexa Fluor 680 or IRDye 800 $F(ab')_2$ for immunoblotting were obtained from LI-COR Biosciences. Alexa Fluor 488–conjugated anti-Rab11 mAb and Alexa Fluor 594–conjugated 20B mAb were produced using conjugation kits (Invitrogen) according to the manufacturer's protocols.

Generation of pSico shRNA lentivirus, stable cell lines, and Cre-induced knockdown of ARH

Target sequences against the mRNA of rat ARH were identified using pSicoOligomaker software (Ventura et al., 2004) and oligonucleotides with the sequences 5′-TACAGTCAGCGCTAATACTATTCAAGAGATAGTATTAGCGCTGACTGTTTTTTTC-3′ (sh3) and 5′-TGAGAACGTGTCCATTTACATTCAAGAGATGTAAATGGACACGTTCTCTTTTTTC-3′ (sh4) as well as their antisense sequences were custom synthesized by Integrated DNA Technologies. The sense and antisense oligos were annealed and then ligated into the pSico-PGK-puro vector (plasmid 11586 from Addgene; Ventura et al., 2004) to obtain pSico-puro-sh3 and pSico-puro-sh4 lentiviral plasmids. A control plasmid (pSico-puro-Luc) designed to express shRNA against luciferase was a gift from Larry Goldstein (University of California, San Diego, La Jolla, CA). Lentiviral particles were prepared using third generation packaging plasmids as described elsewhere (Dull et al., 1998). In brief, 10 µg of the pSico-puro-sh3 and pSico-puro-sh4 plasmids and 10 µg of the lentiviral packaging plasmids were cotransfected into HEK 293T cells using Lipofectamine 2000 (Invitrogen) according to the manufacturer's protocol. After 36 h, the supernatant was collected and used to transduce L2 cells. After 24 h, L2 cells with integrated lentivirus were selected using 5 µg/ml puromycin yielding the L2-Luc, L2-sh3, and L2-sh4 cell lines. shRNA expression was induced with adenovirus carrying Cre recombinase (Ad-Cre; University of Iowa Gene Transfer Vector Core, Iowa City, IA) at MOI 300. 96 h later, cells were either lysed in SDS lysis buffer (50 mM Tris HCl, pH 7.6, 5 mM EDTA, 150 mM NaCl, 1% Triton X-100, and 0.1% SDS) or passaged and used for various assays. Knockdown efficiency was determined by analyzing 25 µg cell lysates by SDS-PAGE and immunoblotting for ARH as described previously (Lehtonen et al., 2008).

Whole-cell lysis and immunoblotting

Cells were harvested, suspended in 2.5× Laemmli sample buffer, and boiled 15 min. Samples were separated by 10% or 5% SDS-PAGE (for megalin analysis) and transferred to PVDF-FL membranes (EMD Millipore). Membranes were blocked in 5% nonfat dry milk and incubated with primary antibodies (4°C overnight), followed by secondary antibodies (1 h at room temperature). Bands were imaged and quantified by two-color detection with the Odyssey infrared imaging system (LI-COR Biosciences). Knockdown efficiency of various proteins was determined by quantifying the reduction in their levels after normalizing for α-tubulin in the same samples.

Plasmid cloning and site-directed mutagenesis

An expression vector for myc-dynein IC2 was a gift from Richard Vallee (Columbia University, New York, NY). Plasmids for expression of recombinant GST-ARH (rARH cloned in frame into the EcoRI–XhoI sites of pGEX-KG) and GST-megalin tail (rat megalin cDNA bases 13341–13980 cloned in frame into the EcoRI–XhoI sites of pGEX-KG) proteins in *Escherichia coli* have been described elsewhere (Nagai et al., 2003). Full-length wt rat ARH and rat dynein IC2C cDNAs were PCR amplified and subcloned into pET24a vector (Takara Bio Inc.) into the NdeI–BamHI sites using standard molecular cloning techniques to yield plasmids for expression of wtARH-His and dynein IC2c-His proteins. Site-directed mutagenesis in these plasmids to yield the various mutants used in this study were done using standard molecular cloning techniques.

Expression and purification of GST-tagged proteins from *E. coli* and GST pull-down assays

Expression of GST-ARH and GST-MT wild-type and mutant proteins in BL21 *E. coli* was induced using 0.3 mM IPTG overnight at 18°C. GST-tagged proteins were purified over a glutathione–Sepharose column as described previously (Nagai et al., 2003; Lehtonen et al., 2008). For pull-down assays, 10 µg GST, GST-MT, or GST-ARH were immobilized on 40 µl glutathione–Sepharose resin (GE Healthcare) for 1 h and then incubated with either 500 µg MEF lysate (for pull-down with GST-MT) or 0.25–10 µg of purified dynein IC2-His protein (for pull-down with GST-ARH) overnight at 4°C. Beads were washed, incubated with SDS sample buffer, and the eluted proteins were analyzed by immunoblotting.

Expression and purification of His-tagged proteins and PTD-NTA delivery of ARH-His proteins

The expression of ARH-His proteins (wt and mutants) and dynein-IC2-His was induced using 0.3 mM IPTG overnight at 18°C in BL21 *E. coli*, and the proteins were then purified on a Ni-NTA resin (QIAGEN) using the manufacturer's guidelines. Intracellular delivery of ARH-His proteins into L2 cells was performed according to June et al. (2010). In brief, 0.6 mM nickel sulfate was incubated with 150 µM PTD-NTA (a gift from Ron June and Steve Dowdy, UCSD) for 5 min. ARH-His protein was added to the mix at a final concentration of 1 µM and incubated for 5 min. The protein–PTD-NTA complex was diluted in serum-free medium and layered on L2-sh3 cells for 90 min. Cells were then washed three times with PBS supplemented with heparin, after which they were either lysed for immunoblotting or used for 20B mAb uptake assays (see below).

Adenovirus-mediated expression of human ARH

Adenoviruses for tetracycline-inducible expression of hARH wt and R266A mutant, in the pACTreCMV backbone (Garuti et al., 2005), were a gift from Helen Hobbs and Jonathan Cohen (University of Texas Southwestern Medical Center, Dallas, TX) and were amplified in HEK 293T cells. L2 cells were washed once with PBS supplemented with 1 mM $MgCl_2$ and transduced with viruses at MOI 50 in serum-free DMEM. After 1 h, the media was removed, and cells were incubated in serum containing DMEM with 0.5 µg/ml doxycycline to induce the expression of hARH. Cells were lysed after 24 h for protein analysis or used for 20B uptake assays.

Plasmid transfection and siRNA delivery using PTD-DRBD

Myc-IC2 plasmid (a gift from Richard Vallee) was transfected into MDCK-M4-ARH cells using Lipofectamine 2000 (Invitrogen) according to the manufacturer's protocol. siRNA duplexes against rat Dab-2 (5′-GCAACAGGCUGAACCAUUAdTdT-3′) and connecdenn2 (5′-GGAAGAGGTTTCTCTGATAdTdT-3′) were obtained from Allele Biotech and were complexed with PTD-DRBD protein and delivered into L2 cells as described by Eguchi et al. (2009). In brief, 60 µl of 50 µM PTD-DRBD (a gift from Akiko Eguchi and Steve Dowdy, UCSD) was mixed with 75 µl PBS, 15 µl of siRNA duplex (20 µM) was added, and the mixture was incubated on ice for 20 min. L2 cells in a 35-mm dish were washed twice with serum-free medium and incubated with 600 µl serum-free medium. The siRNA–PTD-DRBD mix was added to the cells and allowed to incubate for 90 min. The siRNA mix was removed, and cells were incubated in serum containing medium and then either harvested at 48 h for analysis by immunoblotting or trypsinized and replated at 40 h (for 8 h) at a lower density before being used for 20B uptake assays (see below).

Megalin 20B mAb and Texas red–transferrin uptake assays

Megalin 20B mAb uptake studies were performed essentially as described previously (Nagai et al., 2003). In brief, cells grown on coverslips were incubated in serum-free DMEM for 2 h, cooled on ice, and 20B anti-megalin mAb (250 µg/ml) was bound to the cells for 30 min on ice. Cells were rinsed in ice-cold DMEM and either fixed with ice-cold 2% PFA for 30 min (to detect cell surface megalin before initiating endocytosis) or placed in prewarmed, serum-free DMEM at 37°C, and incubated for 2–60 min before fixation. Cells were then processed for IF analysis (see below). For simultaneous 20B and transferrin uptake assays, 100 µg/ml TR-Tf was added to the medium in addition to 20B mAb. To test colocalization between Rab11 and megalin, uptake of Alexa Fluor 594–conjugated 20B was performed in a similar manner as unlabeled 20B, followed by fixation and immunostaining of cells with Alexa Fluor 488–conjugated Rab11 mAb.

Immunofluorescence assays

IF was performed at room temperature as described previously. In brief, cells were fixed with 2% PFA for 30 min, permeabilized with 0.2% Triton X-100 for 10 min, blocked with 5% normal goat serum for 30 min, and incubated for 1 h with primary antibodies and for 1 h with highly cross-adsorbed goat anti–mouse Alexa Fluor 594 and anti–rabbit Alexa Fluor 488 $F(ab')_2$. For 20B mAb uptake assays, anti–mouse Alexa Fluor 594 was used to detect cell surface and internalized megalin. For simultaneous 20B and TR-Tf uptake experiments Alexa Fluor 488 anti–mouse $F(ab')_2$ was used to detect 20B-labeled megalin, and TR-Tf was detected by direct fluorescence. For quantification of megalin trafficking to ERC, 20B and TR-Tf uptake was performed for 15 min. Cells from three independent experiments were counted (100 random fields per condition per experiment, 1–5 cells per field on average). Only cells with TR-Tf accumulated at the ERC and visible 20B labeling were counted and then classified as showing or not showing colocalization between megalin and TR-Tf. The mean, SEM, and Student's *t* test analysis were performed using Microsoft Excel. To visualize Rab35, cells were permeabilized with 0.05% saponin in 80 mM Pipes, pH 6.8, 5 mM EGTA, and 1 mM $MgCl_2$ for 1 min before fixation. Images were acquired with an Ultraview Vox spinning disk confocal microscope (PerkinElmer) using a 63× objective (1.3 NA) and Volocity software. Dark settings for acquired images were adjusted using linear adjustments in Adobe Photoshop CS4.

Immunoelectron microscopy

Control (L2-Luc) and ARH knockdown (L2-sh3) cells loaded with anti-megalin mouse 20B antibody for 60 min were fixed in 2% PFA for 30 min and in 4% PFA for 4 h in 0.1 M phosphate buffer, scraped from the culture dish, and centrifuged before being snap frozen in liquid nitrogen. Ultrathin cryosections (70–80 nm) were labeled with a goat anti–mouse IgG (bridging antibody) for 2 h, followed by a 12-nm gold–conjugated donkey anti–goat IgG for 1 h to visualize internalized megalin. Sections were then contrasted (10 min in 0.4% uranyl acetate and 1.8% methyl cellulose on ice) and imaging was performed using an electron microscope (1200 EX II; JEOL) equipped with an Orius CCD camera (Gatan, Inc.) and digital micrograph software (also from Gatan, Inc.; UCSD Cellular and Molecular Medicine Electron Microscopy Core). For quantification of megalin, ERC areas were selected based on their morphology and proximity to the nucleus and/or centrosome. Gold particles present at the ERC were counted from 17 individual sections for each cell type. Results were expressed as number of gold particles per profile of the ERC, and statistical analysis (mean, SEM, and Student's *t* test) was performed using Microsoft Excel.

Co-immunoprecipitation experiments and peptide displacement assays

MDCK-M4-ARH cells were lysed with Triton lysis buffer (0.5% Triton X-100, 50 mM Tris, pH 7.4, 150 mM NaCl, 5 mM EDTA, 1 mM $MgCl_2$, 1× Complete EDTA-free protease inhibitor, 1 mM Na_3VO_4, and 5 mM NaF), cleared by centrifugation for 15 min at 15,000 *g*, and protein concentration was determined by Bradford assay. Lysate (1 mg protein) was incubated with either 2 µg anti-HA antibody or control mouse IgG overnight at 4°C, after which 30 µl protein G beads were added to the lysates and incubated for 1 h. Beads were washed (3×) with 1 ml Triton lysis buffer and either treated with SDS sample buffer directly or incubated with 10–100 µM of megalin tail peptides (CMEVGKQPVIFENPMYAA or PVIFENPMYAAK), a control peptide, or diluted in Triton lysis buffer for 1 h before adding SDS sample buffer. Samples were boiled and analyzed by SDS-PAGE and immunoblotting.

Biotinylation studies

Biotinylation studies were performed in L2 cells expressing M4-GFP, a mini-megalin receptor that contains its fourth ligand-binding domain (M4) and cytoplasmic tail but lacks ligand binding domains 1–3. L2-Luc or L2-sh3 cells in 60-mm dishes were washed with PBS supplemented with 1 mM $MgCl_2$ and transduced with M4-GFP (MOI = 250) and transactivator TA (MOI = 50) adenoviruses (gifts from Ora Weisz, University of Pittsburgh, Pittsburgh, PA) for 1 h in serum-free medium. The medium was then replaced with DMEM supplemented with 0.5 µg/ml doxycycline and serum. 24 h later, cells were incubated in serum-free medium for 2 h before the start of the biotinylation assay. For surface biotinylation, cells were washed twice with PBS and incubated in 0.5 mg/ml Sulfo-NHS-SS-biotin (Thermo Fisher Scientific) in PBS on ice and then washed once with 50 mM NH_4Cl to quench the unbound biotin. Endocytosis was resumed by adding warm serum-free DMEM supplemented with 5 nM lactoferrin (a natural ligand for megalin) and 50 µg/ml transferrin and incubating cells for 5–15 min at 37°C. Endocytosis was stopped by washing the cells with chilled PBS and placing the plates on ice. Biotin bound to cell surface proteins was stripped by incubating cells in 50 mM MESNA twice for 10 min. Cells were then lysed with 400 µl SDS lysis buffer, and biotinylated proteins were isolated over a NeutrAvidin column (Thermo Fisher Scientific) and analyzed by immunoblotting. For recycling assays, surface-biotinylated proteins were allowed to internalize at 37°C for 10 min, followed by stripping the biotin bound to the cell surface. The cells were again incubated at 37°C in serum-free medium (to allow the internalized biotinylated to recycle back to the PM), and at specified time points (25, 40, and 55 min) the cell surface–biotinylated proteins were once again stripped using MESNA. The biotinylated proteins that did not recycle back to the PM were then isolated on a NeutrAvidin column and analyzed by immunoblotting.

Preparation of membrane and cytosolic fractions

Preparation of membrane and cytosolic fractions was performed as described previously (Beas et al., 2012). L2-Luc and L2-sh3 cells were switched to serum-free DMEM for 2 h, followed by treatment with 5 nM

lactoferrin for 15 min. Cells were scraped and suspended in 3 mM imidazole buffer in 250 mM sucrose and homogenized using a tight Dounce homogenizer. Unbroken cells and nuclei were removed by centrifugation (1,200 *g*, 5 min) and the resulting postnuclear supernatants were centrifuged for 1 h at 100,000 *g* to yield the cytosolic fraction (100,000 *g* supernatant) and the membrane fraction (100,000 *g* pellet), which were resuspended in 2× sample buffer and analyzed by immunoblotting.

RT-PCR

Total RNA was isolated from each cell line using the RNeasy Mini kit (QIAGEN). First-strand cDNA was generated by RT-PCR using 4.5 mg total RNA from each cell line and the Superscript First Strand Synthesis System for RT-PCR (Invitrogen). PCR was performed using the Taq DNA polymerase (New England Biolabs, Inc.) and the following primers (Allele Biotechnology): 5′-TGGAATCTCCCTTGATCCTG-3′ and 5′-TGTTGCTGCCATCAGTCTTC-3′ for megalin, 5′-GGCAAGTTCAATGGCACAGT-3′ and 5′-TGGTGAAGACGCCAGTAGACTC-3′ for glyceraldehyde-3-phosphate dehydrogenase (GAPDH), and 5′-GGAACAGAGGCGGAGGAGCAT-3′ and 5′-GAAGTTGTGTGCCAGATTCTC-3′ for NHE3. The number of cycles and annealing temperature for the PCR were optimized to ensure a single PCR product that was within the linear range. The amplified PCR products were visualized, photographed (Chemi Doc XRS; Bio-Rad Laboratories), and quantified using Quantity One SW software (Bio-Rad Laboratories).

Online supplemental material

Fig. S1 (biotinylation assay) shows that the internalization of megalin is not affected by ARH depletion. Fig. S2 (immunogold electron microscopy) shows that ARH depletion reduces labeling of megalin at the ERC but does not affect the tubular morphology of the ERC. Fig. S3 shows that Y117D, a PTB domain mutation within ARH that perturbs its interaction with megalin, inhibits the trafficking of megalin to the ERC. Fig. S4 shows that adenovirus-mediated expression of ARH restores the trafficking of megalin in ARH-depleted cells. Fig. S5 shows that adenoviral expression of ARH R266A leads to fast recycling of megalin, and it was not able to fully restore its trafficking to the ERC. Online supplemental material is available at http://www.jcb.org/cgi/content/full/jcb.201211110/DC1.

We thank Steve Dowdy, Ron June, and Akiko Eguchi for extensive help with the PTD-NTA and PTD-DRBD techniques; Helen Hobbs and Jonathan Cohen for the hARH adenoviruses; and Ora Weisz for the M4-GFP adenovirus. We thank Pradipta Ghosh, Anthony Beas, and Joann Trejo for useful discussions. Confocal microscopy was carried out at the UCSD Shared Microscopy Facility (National Institutes of Health grant P30 NS047101), and electron microscopy in the UCSD Cellular and Molecular Medicine Electron Microscopy Facility.

This research was supported by a postdoctoral fellowship from the American Heart Association to M. Shah and National Institute of Diabetes and Digestive and Kidney Diseases grant R37 DK17724 to M.G. Farquhar.

Submitted: 20 November 2012
Accepted: 4 June 2013

References

Allaire, P.D., A.L. Marat, C. Dall'Armi, G. Di Paolo, P.S. McPherson, and B. Ritter. 2010. The Connecdenn DENN domain: a GEF for Rab35 mediating cargo-specific exit from early endosomes. *Mol. Cell*. 37:370–382. http://dx.doi.org/10.1016/j.molcel.2009.12.037

Beas, A.O., V. Taupin, C. Teodorof, L.T. Nguyen, M. Garcia-Marcos, and M.G. Farquhar. 2012. Gαs promotes EEA1 endosome maturation and shuts down proliferative signaling through interaction with GIV (Girdin). *Mol. Biol. Cell*. 23:4623–4634. http://dx.doi.org/10.1091/mbc.E12-02-0133

Birn, H., and E.I. Christensen. 2006. Renal albumin absorption in physiology and pathology. *Kidney Int.* 69:440–449. http://dx.doi.org/10.1038/sj.ki.5000141

Christensen, E.I., and H. Birn. 2002. Megalin and cubilin: multifunctional endocytic receptors. *Nat. Rev. Mol. Cell Biol.* 3:256–266.

Christensen, E.I., and P.J. Verroust. 2002. Megalin and cubilin, role in proximal tubule function and during development. *Pediatr. Nephrol.* 17:993–999. http://dx.doi.org/10.1007/s00467-002-0956-5

Cui, S., P.J. Verroust, S.K. Moestrup, and E.I. Christensen. 1996. Megalin/gp330 mediates uptake of albumin in renal proximal tubule. *Am. J. Physiol.* 271:F900–F907.

Czekay, R.P., R.A. Orlando, L. Woodward, E.D. Adamson, and M.G. Farquhar. 1995. The expression of megalin (gp330) and LRP diverges during F9 cell differentiation. *J. Cell Sci.* 108:1433–1441.

Daro, E., P. van der Sluijs, T. Galli, and I. Mellman. 1996. Rab4 and cellubrevin define different early endosome populations on the pathway of transferrin receptor recycling. *Proc. Natl. Acad. Sci. USA*. 93:9559–9564. http://dx.doi.org/10.1073/pnas.93.18.9559

Davis, C.G., M.A. Lehrman, D.W. Russell, R.G. Anderson, M.S. Brown, and J.L. Goldstein. 1986. The J.D. mutation in familial hypercholesterolemia: amino acid substitution in cytoplasmic domain impedes internalization of LDL receptors. *Cell*. 45:15–24. http://dx.doi.org/10.1016/0092-8674(86)90533-7

De Strooper, B., and W. Annaert. 2010. Novel research horizons for presenilins and γ-secretases in cell biology and disease. *Annu. Rev. Cell Dev. Biol.* 26:235–260. http://dx.doi.org/10.1146/annurev-cellbio-100109-104117

Dull, T., R. Zufferey, M. Kelly, R.J. Mandel, M. Nguyen, D. Trono, and L. Naldini. 1998. A third-generation lentivirus vector with a conditional packaging system. *J. Virol.* 72:8463–8471.

Dumanchin, C., C. Czech, D. Campion, M.H. Cuif, T. Poyot, C. Martin, F. Charbonnier, B. Goud, L. Pradier, and T. Frebourg. 1999. Presenilins interact with Rab11, a small GTPase involved in the regulation of vesicular transport. *Hum. Mol. Genet.* 8:1263–1269. http://dx.doi.org/10.1093/hmg/8.7.1263

Dvir, H., M. Shah, E. Girardi, L. Guo, M.G. Farquhar, and D.M. Zajonc. 2012. Atomic structure of the autosomal recessive hypercholesterolemia phosphotyrosine-binding domain in complex with the LDL-receptor tail. *Proc. Natl. Acad. Sci. USA*. 109:6916–6921. http://dx.doi.org/10.1073/pnas.1114128109

Egami, Y., M. Fukuda, and N. Araki. 2011. Rab35 regulates phagosome formation through recruitment of ACAP2 in macrophages during FcγR-mediated phagocytosis. *J. Cell Sci.* 124:3557–3567. http://dx.doi.org/10.1242/jcs.083881

Eguchi, A., B.R. Meade, Y.C. Chang, C.T. Fredrickson, K. Willert, N. Puri, and S.F. Dowdy. 2009. Efficient siRNA delivery into primary cells by a peptide transduction domain-dsRNA binding domain fusion protein. *Nat. Biotechnol.* 27:567–571. http://dx.doi.org/10.1038/nbt.1541

Fang, L., R. Garuti, B.Y. Kim, J.B. Wade, and P.A. Welling. 2009. The ARH adaptor protein regulates endocytosis of the ROMK potassium secretory channel in mouse kidney. *J. Clin. Invest.* 119:3278–3289.

Garcia, C.K., K. Wilund, M. Arca, G. Zuliani, R. Fellin, M. Maioli, S. Calandra, S. Bertolini, F. Cossu, N. Grishin, et al. 2001. Autosomal recessive hypercholesterolemia caused by mutations in a putative LDL receptor adaptor protein. *Science*. 292:1394–1398. http://dx.doi.org/10.1126/science.1060458

Garuti, R., C. Jones, W.P. Li, P. Michaely, J. Herz, R.D. Gerard, J.C. Cohen, and H.H. Hobbs. 2005. The modular adaptor protein autosomal recessive hypercholesterolemia (ARH) promotes low density lipoprotein receptor clustering into clathrin-coated pits. *J. Biol. Chem.* 280:40996–41004. http://dx.doi.org/10.1074/jbc.M509394200

Goody, R.S., A. Rak, and K. Alexandrov. 2005. The structural and mechanistic basis for recycling of Rab proteins between membrane compartments. *Cell. Mol. Life Sci.* 62:1657–1670. http://dx.doi.org/10.1007/s00018-005-4486-8

Grant, B.D., and J.G. Donaldson. 2009. Pathways and mechanisms of endocytic recycling. *Nat. Rev. Mol. Cell Biol.* 10:597–608. http://dx.doi.org/10.1038/nrm2755

Hanyaloglu, A.C., and M. von Zastrow. 2008. Regulation of GPCRs by endocytic membrane trafficking and its potential implications. *Annu. Rev. Pharmacol. Toxicol.* 48:537–568. http://dx.doi.org/10.1146/annurev.pharmtox.48.113006.094830

He, G., S. Gupta, M. Yi, P. Michaely, H.H. Hobbs, and J.C. Cohen. 2002. ARH is a modular adaptor protein that interacts with the LDL receptor, clathrin, and AP-2. *J. Biol. Chem.* 277:44044–44049. http://dx.doi.org/10.1074/jbc.M208539200

Hsu, V.W., and R. Prekeris. 2010. Transport at the recycling endosome. *Curr. Opin. Cell Biol.* 22:528–534. http://dx.doi.org/10.1016/j.ceb.2010.05.008

Hsu, V.W., M. Bai, and J. Li. 2012. Getting active: protein sorting in endocytic recycling. *Nat. Rev. Mol. Cell Biol.* 13:323–328. http://dx.doi.org/10.1038/nrm3272

Jones, C., R.E. Hammer, W.P. Li, J.C. Cohen, H.H. Hobbs, and J. Herz. 2003. Normal sorting but defective endocytosis of the low density lipoprotein receptor in mice with autosomal recessive hypercholesterolemia. *J. Biol. Chem.* 278:29024–29030. http://dx.doi.org/10.1074/jbc.M304855200

June, R.K., K. Gogoi, A. Eguchi, X.S. Cui, and S.F. Dowdy. 2010. Synthesis of a pH-sensitive nitrilotriacetic linker to peptide transduction domains to enable intracellular delivery of histidine imidazole ring-containing macromolecules. *J. Am. Chem. Soc.* 132:10680–10682. http://dx.doi.org/10.1021/ja1040418

Kantarci, S., L. Al-Gazali, R.S. Hill, D. Donnai, G.C. Black, E. Bieth, N. Chassaing, D. Lacombe, K. Devriendt, A. Teebi, et al. 2007. Mutations in

LRP2, which encodes the multiligand receptor megalin, cause Donnai-Barrow and facio-oculo-acoustico-renal syndromes. *Nat. Genet.* 39:957–959. http://dx.doi.org/10.1038/ng2063

Kardon, J.R., and R.D. Vale. 2009. Regulators of the cytoplasmic dynein motor. *Nat. Rev. Mol. Cell Biol.* 10:854–865. http://dx.doi.org/10.1038/nrm2804

Kaup, M., K. Dassler, C. Weise, and H. Fuchs. 2002. Shedding of the transferrin receptor is mediated constitutively by an integral membrane metalloprotease sensitive to tumor necrosis factor alpha protease inhibitor-2. *J. Biol. Chem.* 277:38494–38502. http://dx.doi.org/10.1074/jbc.M203461200

Kelly, B.T., and D.J. Owen. 2011. Endocytic sorting of transmembrane protein cargo. *Curr. Opin. Cell Biol.* 23:404–412. http://dx.doi.org/10.1016/j.ceb.2011.03.004

Keyel, P.A., S.K. Mishra, R. Roth, J.E. Heuser, S.C. Watkins, and L.M. Traub. 2006. A single common portal for clathrin-mediated endocytosis of distinct cargo governed by cargo-selective adaptors. *Mol. Biol. Cell*. 17:4300–4317. http://dx.doi.org/10.1091/mbc.E06-05-0421

Kopan, R., and M.X. Ilagan. 2004. Gamma-secretase: proteasome of the membrane? *Nat. Rev. Mol. Cell Biol.* 5:499–504. http://dx.doi.org/10.1038/nrm1406

Kouranti, I., M. Sachse, N. Arouche, B. Goud, and A. Echard. 2006. Rab35 regulates an endocytic recycling pathway essential for the terminal steps of cytokinesis. *Curr. Biol.* 16:1719–1725. http://dx.doi.org/10.1016/j.cub.2006.07.020

Laporte, S.A., R.H. Oakley, J.A. Holt, L.S. Barak, and M.G. Caron. 2000. The interaction of beta-arrestin with the AP-2 adaptor is required for the clustering of beta 2-adrenergic receptor into clathrin-coated pits. *J. Biol. Chem.* 275:23120–23126. http://dx.doi.org/10.1074/jbc.M002581200

Leheste, J.R., B. Rolinski, H. Vorum, J. Hilpert, A. Nykjaer, C. Jacobsen, P. Aucouturier, J.O. Moskaug, A. Otto, E.I. Christensen, and T.E. Willnow. 1999. Megalin knockout mice as an animal model of low molecular weight proteinuria. *Am. J. Pathol.* 155:1361–1370. http://dx.doi.org/10.1016/S0002-9440(10)65238-8

Lehtonen, S., M. Shah, R. Nielsen, N. Iino, J.J. Ryan, H. Zhou, and M.G. Farquhar. 2008. The endocytic adaptor protein ARH associates with motor and centrosomal proteins and is involved in centrosome assembly and cytokinesis. *Mol. Biol. Cell*. 19:2949–2961. http://dx.doi.org/10.1091/mbc.E07-05-0521

Li, Y., R. Cong, and D. Biemesderfer. 2008. The COOH terminus of megalin regulates gene expression in opossum kidney proximal tubule cells. *Am. J. Physiol. Cell Physiol.* 295:C529–C537. http://dx.doi.org/10.1152/ajpcell.00037.2008

Marat, A.L., and P.S. McPherson. 2010. The connecdenn family, Rab35 guanine nucleotide exchange factors interfacing with the clathrin machinery. *J. Biol. Chem.* 285:10627–10637. http://dx.doi.org/10.1074/jbc.M109.050930

Maurer, M.E., and J.A. Cooper. 2006. The adaptor protein Dab2 sorts LDL receptors into coated pits independently of AP-2 and ARH. *J. Cell Sci.* 119:4235–4246. http://dx.doi.org/10.1242/jcs.03217

Maxfield, F.R., and T.E. McGraw. 2004. Endocytic recycling. *Nat. Rev. Mol. Cell Biol.* 5:121–132. http://dx.doi.org/10.1038/nrm1315

McMahon, H.T., and E. Boucrot. 2011. Molecular mechanism and physiological functions of clathrin-mediated endocytosis. *Nat. Rev. Mol. Cell Biol.* 12:517–533. http://dx.doi.org/10.1038/nrm3151

Miettinen, A., G. Dekan, and M.G. Farquhar. 1990. Monoclonal antibodies against membrane proteins of the rat glomerulus. Immunochemical specificity and immunofluorescence distribution of the antigens. *Am. J. Pathol.* 137:929–944.

Mishra, S.K., S.C. Watkins, and L.M. Traub. 2002. The autosomal recessive hypercholesterolemia (ARH) protein interfaces directly with the clathrin-coat machinery. *Proc. Natl. Acad. Sci. USA*. 99:16099–16104. http://dx.doi.org/10.1073/pnas.252630799

Mishra, S.K., P.A. Keyel, M.A. Edeling, A.L. Dupin, D.J. Owen, and L.M. Traub. 2005. Functional dissection of an AP-2 beta2 appendage-binding sequence within the autosomal recessive hypercholesterolemia protein. *J. Biol. Chem.* 280:19270–19280. http://dx.doi.org/10.1074/jbc.M501029200

Morris, S.M., S.D. Arden, R.C. Roberts, J. Kendrick-Jones, J.A. Cooper, J.P. Luzio, and F. Buss. 2002. Myosin VI binds to and localises with Dab2, potentially linking receptor-mediated endocytosis and the actin cytoskeleton. *Traffic*. 3:331–341. http://dx.doi.org/10.1034/j.1600-0854.2002.30503.x

Nagai, J., E.I. Christensen, S.M. Morris, T.E. Willnow, J.A. Cooper, and R. Nielsen. 2005. Mutually dependent localization of megalin and Dab2 in the renal proximal tubule. *Am. J. Physiol. Renal Physiol.* 289:F569–F576. http://dx.doi.org/10.1152/ajprenal.00292.2004

Nagai, M., T. Meerloo, T. Takeda, and M.G. Farquhar. 2003. The adaptor protein ARH escorts megalin to and through endosomes. *Mol. Biol. Cell*. 14:4984–4996. http://dx.doi.org/10.1091/mbc.E03-06-0385

Oleinikov, A.V., J. Zhao, and S.P. Makker. 2000. Cytosolic adaptor protein Dab2 is an intracellular ligand of endocytic receptor gp600/megalin. *Biochem. J.* 347:613–621. http://dx.doi.org/10.1042/0264-6021:3470613

Orlando, R.A., and M.G. Farquhar. 1993. Identification of a cell line that expresses a cell surface and a soluble form of the gp330/receptor-associated protein (RAP) Heymann nephritis antigenic complex. *Proc. Natl. Acad. Sci. USA*. 90:4082–4086. http://dx.doi.org/10.1073/pnas.90.9.4082

Palmer, K.J., H. Hughes, and D.J. Stephens. 2009. Specificity of cytoplasmic dynein subunits in discrete membrane-trafficking steps. *Mol. Biol. Cell*. 20:2885–2899. http://dx.doi.org/10.1091/mbc.E08-12-1160

Pfeffer, S., and D. Aivazian. 2004. Targeting Rab GTPases to distinct membrane compartments. *Nat. Rev. Mol. Cell Biol.* 5:886–896. http://dx.doi.org/10.1038/nrm1500

Platta, H.W., and H. Stenmark. 2011. Endocytosis and signaling. *Curr. Opin. Cell Biol.* 23:393–403. http://dx.doi.org/10.1016/j.ceb.2011.03.008

Ren, M., G. Xu, J. Zeng, C. De Lemos-Chiarandini, M. Adesnik, and D.D. Sabatini. 1998. Hydrolysis of GTP on rab11 is required for the direct delivery of transferrin from the pericentriolar recycling compartment to the cell surface but not from sorting endosomes. *Proc. Natl. Acad. Sci. USA*. 95:6187-6192.

Saito, A., S. Pietromonaco, A.K. Loo, and M.G. Farquhar. 1994. Complete cloning and sequencing of rat gp330/"megalin," a distinctive member of the low density lipoprotein receptor gene family. *Proc. Natl. Acad. Sci. USA*. 91:9725–9729. http://dx.doi.org/10.1073/pnas.91.21.9725

Scita, G., and P.P. Di Fiore. 2010. The endocytic matrix. *Nature*. 463:464–473. http://dx.doi.org/10.1038/nature08910

Skikne, B.S., C.H. Flowers, and J.D. Cook. 1990. Serum transferrin receptor: a quantitative measure of tissue iron deficiency. *Blood*. 75:1870–1876.

Traer, C.J., A.C. Rutherford, K.J. Palmer, T. Wassmer, J. Oakley, N. Attar, J.G. Carlton, J. Kremerskothen, D.J. Stephens, and P.J. Cullen. 2007. SNX4 coordinates endosomal sorting of TfnR with dynein-mediated transport into the endocytic recycling compartment. *Nat. Cell Biol.* 9:1370–1380. http://dx.doi.org/10.1038/ncb1656

Traub, L.M. 2009. Tickets to ride: selecting cargo for clathrin-regulated internalization. *Nat. Rev. Mol. Cell Biol.* 10:583–596. http://dx.doi.org/10.1038/nrm2751

Ullrich, O., S. Reinsch, S. Urbé, M. Zerial, and R.G. Parton. 1996. Rab11 regulates recycling through the pericentriolar recycling endosome. *J. Cell Biol.* 135:913–924. http://dx.doi.org/10.1083/jcb.135.4.913

Ventura, A., A. Meissner, C.P. Dillon, M. McManus, P.A. Sharp, L. Van Parijs, R. Jaenisch, and T. Jacks. 2004. Cre-lox-regulated conditional RNA interference from transgenes. *Proc. Natl. Acad. Sci. USA*. 101:10380–10385. http://dx.doi.org/10.1073/pnas.0403954101

Walseng, E., O. Bakke, and P.A. Roche. 2008. Major histocompatibility complex class II-peptide complexes internalize using a clathrin- and dynamin-independent endocytosis pathway. *J. Biol. Chem.* 283:14717–14727. http://dx.doi.org/10.1074/jbc.M801070200

Willnow, T.E., J. Hilpert, S.A. Armstrong, A. Rohlmann, R.E. Hammer, D.K. Burns, and J. Herz. 1996. Defective forebrain development in mice lacking gp330/megalin. *Proc. Natl. Acad. Sci. USA*. 93:8460–8464. http://dx.doi.org/10.1073/pnas.93.16.8460

Zhang, M., A. Haapasalo, D.Y. Kim, L.A. Ingano, W.H. Pettingell, and D.M. Kovacs. 2006. Presenilin/gamma-secretase activity regulates protein clearance from the endocytic recycling compartment. *FASEB J.* 20:1176–1178. http://dx.doi.org/10.1096/fj.05-5531fje

Zou, Z., B. Chung, T. Nguyen, S. Mentone, B. Thomson, and D. Biemesderfer. 2004. Linking receptor-mediated endocytosis and cell signaling: evidence for regulated intramembrane proteolysis of megalin in proximal tubule. *J. Biol. Chem.* 279:34302–34310. http://dx.doi.org/10.1074/jbc.M405608200